Review on Estimation of Land Surface Radiation and Energy Budgets From Ground Measurement, Remote Sensing and Model Simulations

Shunlin Liang, *Senior Member, IEEE*, Kaicun Wang, Xiaotong Zhang, and Martin Wild

***Abstract*—Land surface radiation and energy budgets are critical components of any land surface models that characterize hydrological, ecological and biogeochemical processes. The estimates of their components generated from remote sensing data or simulations from numerical models have large uncertainties. This paper provides a comprehensive review of recent advances in estimating insolation, albedo, clear-sky longwave downward and upwelling radiation, all-wave net radiation and evapotranspiration from ground measurements, remote sensing algorithms and products, as well as numerical model simulations. The decadal variations of these components are also discussed.**

***Index Terms*—Energy budget, evapotranspiration, model simulation, net radiation, radiation budget, remote sensing.**

I. Introduction

LAND surface energy balance is central to any land models that characterize the land surface processes (e.g., ecological, hydrological, biogeochemical). The land surface energy balance equation can be written as

$$R_n = G + H + \lambda ET \tag{1}$$

where R_n is all-wave net radiation, G is soil heat flux, H is sensible heat flux, and λET is latent heat flux in which λ is the latent heat of evaporation of water and ET is the rate of evaporation of water.

The land surface radiation budget, characterized by the net radiation, represents the balance between incoming radiation from the atmosphere and outgoing longwave and reflected shortwave radiation from the Earth surfaces. All-wave net radiation is the sum of shortwave net radiation (R_n^s) and longwave net radiation (R_n^l), and can be expressed by

$$\begin{cases} R_n = R_n^s + R_n^l & (2)\\ R_n^s = (1-\alpha)F_d^s & (3)\\ R_n^l = F_d^l - F_u^l = \varepsilon F_d^l - \sigma\varepsilon T_s^4 & (4) \end{cases}$$

where α is land surface broadband albedo, F_d^s and F_d^l are the shortwave and longwave downward fluxes, F_d^s is often called insolation, F_u^l is longwave upwelling radiation, ε is the broadband emissivity, T_s is the surface skin temperature, and σ is Stefan-Boltzmann's constant.

Due to space limitations in this paper, we focus mainly on the following components: all-sky insolation, albedo, clear-sky longwave downward radiation, clear-sky longwave upwelling radiation, all-wave all-sky net radiation, and evapotranspiration (ET).

II. Insolation

Incident solar radiation, either photosynthetically active radiation (PAR) in the visible spectrum (400–700 nm) or insolation in the total shortwave (300–4000 nm), is a key variable required by almost all land surface models. Many ecosystem models calculate biomass accumulation linearly proportional to incident PAR [1], [2]. Many models for calculating land surface ET are also linearly related to insolation [3], [4].

Insolation is a measure of solar radiation received on a given surface area in a given time, commonly expressed as average irradiance in watts per square meter $(\mathrm{W/m^2})$. Insolation is extraterrestrial irradiance at the top of the atmosphere (TOA) modified by the solar scattering and absorption of the different components of the atmosphere, including Rayleigh scattering, permanent gas absorption, absorption by water vapor, and the absorption and scattering by aerosols and cloud components, respectively. The cloud amount and aerosol loadings are the primary factors.

A. Ground Measurements

Since 1964, measurements of insolation and other components of the surface radiation balance have been published by the World Meteorological Organization (WMO). The meteorological stations in most countries measure insolation.

There are several major measurement networks for radiation measurements—the Global Energy Balance Archive (GEBA) [5]; the Baseline Surface Radiation Network (BSRN) [6]; the

Manuscript received July 14, 2009; revised March 01, 2010 and April 02, 2010; accepted April 06, 2010. Date of publication May 18, 2010; date of current version August 25, 2010. This work was supported in part by the National Aeronautics and Space Administration under Grant NNG05GD10G, the National Oceanic and Atmospheric Administration under Grant NA07NES4400001, and the GOES-R Program.

S. Liang is with the Department of Geography, University of Maryland, College Park, MD 20742 USA, and also with the College of Global Change and Earth System Science, Beijing Normal University, Beijing 100875, China (e-mail: sliang@umd.edu).

K. Wang is with the Department of Geological Science, University of Texas at Austin, Austin, TX 78712 USA.

X. Zhang is with the School of Resource and Environmental Science, Wuhan University, and also with the College of Global Change and Earth System Science, Beijing Normal University, Beijing 100875, China.

M. Wild is with the Institute for Atmospheric and Climate Science, ETH Zurich, Zurich, Switzerland.

Color versions of one or more of the figures in this paper are available online at http://ieeexplore.ieee.org.

Digital Object Identifier 10.1109/JSTARS.2010.2048556

1939-1404/$26.00 © 2010 IEEE

Surface Radiation Budget Network (SURFRAD) [7], [8], and FLUXNET [9].

GEBA is a database maintained by ETH Zurich for the worldwide measured radiation fluxes at the Earth's surface. It currently contains 2,000+ stations with 250,000 monthly mean values of various surface energy balance components collected since the 1950s. Gilgen *et al.* [10] estimated the relative random error (root mean square error (RMSE)/mean) of the incoming shortwave radiation values in GEBA at 5% for the monthly means and 2% for yearly means.

BSRN became operational in 1992 and provides radiation measurements with the highest possible accuracy at high temporal resolution (minute values) in various climate zones. At present, there are 35 BSRN stations in operation. The measurement accuracy is about 5 Wm^{-2} for the total insolation, but 2 Wm^{-2} and 5 Wm^{-2} for the direct and diffuse components, respectively [6].

Established in 1993 by the U. S. National Oceanic and Atmospheric Administration (NOAA) to support climate research over the United States, SURFRAD currently operates seven stations in climatologically diverse regions. Independent measures of upwelling and downwelling solar and infrared are the primary measurements; ancillary observations include direct and diffuse solar radiation, PAR, spectral solar radiation, and meteorological parameters. Data are distributed in near real time by anonymous FTP and the WWW (http://www.srrb.noaa.gov). The documented measurement relative error ranges from $\pm 2\%$ to $\pm 5\%$ [7].

FLUXNET is a global network of micrometeorological tower sites that use eddy covariance methods to measure the exchanges of carbon dioxide, water vapor, and energy between terrestrial ecosystems and the atmosphere. It consists of a set of regional networks, such as AmeriFlux, CarboEurope, AsiaFlux, KoFlux, OzFlux, Fluxnet-Canada, and Chinaflux. As of July 2009, over 500 tower sites are operating on a long-term and continuous basis with the earliest sites dating from 1996. Because of multiple instruments operated in different countries, the accuracies of insolation measurements have not been well documented.

In addition, a number of regional networks exist, for example, the Atmospheric Radiation Measurement (ARM) Program created in 1989 with data available at http://www.arm.gov/docs/data.html; GEWEX Asian Monsoon Experiment (GAME/AAN), the most reliable one for regions at higher elevations [11], Greenland Climate Network (GC-Net) for the Greenland ground measurements with instrument accuracy of 5–15%; and the Aerosol Robotic Network (AERONET) which overestimates radiation parameters by 6 ± 13 Wm^{-2} in the Amazon area [12].

To insure high quality of the collected data, most of the projects selected used Kipp & Zonen or Eppley standard pyranometers and pyrgeometers to measure shortwave and longwave radiation. The uncertainties of the instantaneous values of solar shortwave radiation range from 5–20 Wm^{-2}. The uncertainties of the derived daily or monthly values are expected to be much less [10]. The stated uncertainty of longwave radiation (pyrgeometers) is about 5% or 10–20 Wm^{-2}, and the uncertainties of daily or monthly values are much less. However, the performance of pyranometers and pyrgeometers depends on their calibration, especially for pyrgeometers. The symmetrical errors of longwave radiation of some FLUXNET sites may be more than 10 Wm^{-2} [13].

B. Remote Sensing Techniques

1) Satellite Sensors: Since 1960, meteorological satellites have dramatically advanced our knowledge of the Earth radiation budget. In contrast to ground-based observations, space-borne observations have the advantage of global coverage. The typical broadband radiometers include the Earth Radiation Budget (ERB) sensors aboard Nimbus-7 [14], the Earth Radiation Budget Experiment (ERBE) sensors aboard three satellites [15], Clouds and the Earth's Radiant Energy System (CERES) [16], and the Geostationary Earth Radiation Budget (GERB) sensors carried by Meteosat-8 launched in 2002 and Meteosat-9 launched in 2007 [17]. Note that satellite instruments aim to be well calibrated, but some missions did not have onboard calibration devices, and those that did had to deal with complicated calibration issues related to the changing of onboard optical devices over time.

Besides calibration, there exist significant gaps between these missions, for example the eight years between ERBE and CERES. The multispectral sensors on both polar-orbiting or geostationary satellites also have been used to produce surface radiation products, such as the Spinning Enhanced Visible and Infrared Imager (SEVIRI) radiometers onboard the METEOSAT Second Generation (MSG) satellites [18], Geostationary Operational Environmental Satellites (GOES) [19], the ABI to be carried by GOES-R [20], and the Moderate Resolution Imaging Spectroradiometer (MODIS) [21].

Earlier reviews by Schmetz [22] and Pinker *et al.* [23] revealed that daily insolation estimates from geostationary satellite data are generally within 10%–15% of pyranometer data, while hourly estimates have errors that range from 5%–10% for clear-sky conditions to 15%–30% for all-sky conditions. More recent studies employing data from several different satellites have improved accuracy, but further improvements are needed.

2) Estimation Algorithms: There are roughly two types of algorithms for calculating insolation. **The first approach** is to use the retrieved cloud and atmosphere parameters from other sources, with measured TOA radiance/flux acting as a constraint. They have been used for estimating insolation from CERES, the International Satellite Cloud Climatology Project (ISCCP), and SEVIRI.

The CERES algorithm [16] uses the cloud and aerosol information from MODIS, and TOA broadband fluxes as a constraint, to produce both insolation and PAR at a spatial resolution of 25 km for the instantaneous sensor footprint and 140 km gridded products. Our recent validation results [24] using extensive ground measurements show the 3-hour product has a mean bias of 29.7 Wm^{-2} (6.0% in relative value), and a standard deviation (STD) of 123.2 Wm^{-2} (25.1% in relative value).

The first global shortwave radiation budget data set mainly from ERBE/ERB has a spatial resolution of 280 km and daily temporal resolution, with the bias between ± 20 Wm^{-2} and

RMSE around 25 Wm^{-2} globally, and much larger uncertainties locally [25].

ISCCP has produced a global radiative flux data product called ISCCP FD every three hours from 1983–2006 on a 280 km equal-area global grid [26]. ISCCP FD has been calculated using a radiative transfer model from the Goddard Institute for Space Studies (GISS) General Circulation Model (GCM) using atmosphere and surface properties obtained primarily from the TIROS Operational Vertical Sounding (TOVS) data. The technical details are described by Zhang *et al.* [26] who estimated that the error of this data set is on the order of 10–15 Wm^{-2}. Raschke *et al.* [27] found serious errors in the input data that affect the surface radiation significantly. The recent validation results [24] showed that the three-hour product has a mean bias of 2.8 Wm^{-2} (0.3% in relative value) and an STD of 101.7 Wm^{-2} (35.0% in relative error).

Deneke *et al.* [28] estimated surface solar irradiance based on METEOSAT SEVIRI-derived cloud properties together with data on water vapor column and surface albedo. Their validation results over the Netherlands with one year of pyranometer measurements from 35 stations showed that the residual standard deviations from the linear regression analysis are 56, 11, and 4 Wm^{-2} for hourly, daily and monthly mean irradiance, respectively.

The second approach is to establish the relationship between the TOA radiance and surface incident insolation based on extensive radiative transfer simulations. This method was first applied to analyze the ERBE data [29], [30]. Liang *et al.* [21], [31] generated the PAR and insolation products from MODIS data directly. A similar approach has been used for GOES [32] and AVHRR [33].

The Global Energy and Water Cycle Experiment (GEWEX) surface radiation budget (SRB) Release 2 product has a spatial resolution of $1^\circ \times 1^\circ$ and high temporal resolutions mainly from GOES data [34]. Yang *et al.* [11] compared both ISCCP-FD and GEWEX SRB data sets over the Tibetan Plateau and found large discrepancies among them in highly variable terrain (such as in the Himalayas region). In their official Web site, the shortwave radiation products have biases of -6.64 (3-hourly), -3.67 (daily), and -4.09 (monthly) Wm^{-2}, and an RMSE of 87.87 (3-hourly), 35.14 (daily) and 18.08 (monthly) Wm^{-2}. Our recent validation results using extensive ground measurements [24] show that the three-hour product has a mean bias of -5.5 Wm^{-2} (-1.9% in relative value) and an STD of 101.3 Wm^{-2} (35.0% in relative error).

Diak and Gautier [35] developed a simplified GEWEX algorithm and produced hourly and daily insolation products over the continental United States from GOES data. Compared to pyranometer measurements at 11 sites in the U.S. Climate Reference Network (USCRN) over a continuous 15-month period, the validation results [36] showed seasonally averaged model errors of 62 (19%) and 15 (10%) Wm^{-2} for hourly and daily-averaged insolation, respectively, including both clear- and cloudy-sky conditions. Their daily integrated insolation is available online at http://www.soils.wisc.edu/wimnext/sun.html. Hourly data over the continental United States back to 2002 can be obtained upon request.

The Satellite Application Facility on Climate Monitoring (CM-SAF), part of EUMETSAT's SAF Network, produces the insolation product from AVHRR data [37] using a look-up table (LUT) approach [38]. The product starts beginning Jan. 2004 with a spatial resolution of 15 km and daily and monthly temporal resolutions. The LUT algorithm applies a pre-calculated cloud mask, cloud top pressure and cloud type as inputs to the LUT algorithm [38]. Validation of the instantaneous satellite derived data versus hourly averaged surface measurements of insolation showed good agreement within the targeted accuracy of 10 Wm^{-2} for monthly averages.

C. GCM Simulations

All atmospheric GCMs calculate incident insolation within the atmosphere and at the surface. The generated products usually have much coarser spatial resolutions ($> 1^\circ$) and fine temporal resolutions (six hours).

Most GCMs tend to overestimate surface insolation. Excessive surface insolation has been a long standing problem in GCMs, and is still present in state-of-the-art GCMs [39]. Overestimates are particularly pronounced in lower latitudes in a majority of models. This is in line with evidence from earlier models in which a lack of adequate representation of absorbing aerosol, particularly from biomass burning and desert dust prevailing in lower latitudes, can cause significant overestimation in surface insolation [40]. Bodas-Salcedo *et al.* [41] validated the insolation of the surface radiation budget in the atmospheric component of the new Hadley Centre Global Environmental Model version 1 (HadGEM1) using the BSRN and ISCCP-FD data sets and showed that this model also tends to overestimate the surface incoming solar radiation.

Wild [39] compared the 14 GCMs of the latest generation used in the fourth assessment report of the Intergovernmental Panel on Climate Change (IPCC-AR4) and the 3rd phase of the Coupled Model Intercomparison Project (CMIP3) with a comprehensive data set of 760 GEBA stations. The mean bias amounts to $+6$ Wm^{-2}, with a range from -12 to $+29$ Wm^{-2}.

Xia *et al.* [42], [43] found that the National Center for Environment Prediction (NCEP) reanalysis solar radiation data exceeded surface observations by 40 to 100 (or greater) Wm^{-2}. Zhao *et al.* [44] evaluated three reanalysis data sets (NASA Data Assimilation Office, European Centre for Medium-Range Weather Forecasts (ECMWF) (ERA-40) and NCEP/National Center for Atmospheric Research (NCEP/NCAR) reanalysis) and their impacts on the MODIS net primary productivity (NPP) product. They found that the NCEP reanalysis also tends to overestimate surface solar radiation, ECMWF has the highest accuracy but its radiation is lower in tropical regions, and the accuracy of DAO lies between that of NCEP and ECMWF.

Table I shows the average insolation estimates over land surfaces from several sources. The first seven columns were extracted from two papers, where NRA, JRA and ERA-40 are reanalysis data, and the last two columns are calculated in this study.

D. Decadal Variations

Analysis of long-term GEBA measurements [45]–[47] showed that the insolation undergoes significant decadal vari-

TABLE I
ESTIMATED AVERAGED INSOLATION OVER LAND SURFACES (Wm^{-2})

dataset	ISCCP-FD [163]	NRA [163]	ERA-40 [163]	JRA [163]	Trenberth et al. [163]	GEBA* mean [178]	IPCC AR4 GCM mean	GEWEX
Feb. 1985-April 1989	190.1	224.1	177.2	206.4		169	191	
Mar 2000 – May 2004	188.8	225.4	-	207.4	184.7			182.4

*mean value at 760 stations.

ations. The record of observed global radiation begins with an increasing phase from the 1920s to the late 1940s/early 1960s. This brightening period (first brightening phase) is followed by a decreasing trend lasting to the late 1980s, known as the global dimming, which finally transitions into the second brightening phase in many regions of the world. Wang *et al.* (in preparation) using globally available meteorological visibility inverse aerosol optical depth and sunshine duration measurements showed that dimming of insolation renewed over Europe after 2004, over Southeast Asia and Middle Asia after 2000, after 1995 over China, and after 1989 over India. The decadal variations of insolation are highly correlated with cloud coverage and aerosol loadings.

However, the studies on utilizing GEBA data have been challenged because the sparse surface point measurements have an obvious urban bias [48]. Satellite-derived insolation has good global coverage, but current long-term satellite estimated insolation data often contain spurious changes resulting from satellite changes, sensor calibration, satellite view geometry [49] and the difficulty in incorporating long-term variation in atmospheric aerosols [11], [50]. Evan *et al.* [49] suggested that the ISCCP data in its current form may be inappropriate for certain long-term global studies, especially those focused on trends. The state-of-the-art GCMs have not been able to characterize decadal variations well [40].

Global "brightening" and "dimming" has great implications for climate change [51]–[54] and hydrological cycles [55]. In the IPCC-AR4, continental- and global-scale surface temperatures are shown to decrease slightly from the 1950s to the 1970s, but drastically increase since the 1980s, with strongest temperature rises on northern continents. This kind of behavior matches the similar patterns of the decadal variations of insolation.

III. SHORTWAVE ALBEDO

Land surface albedo modulates the amount of solar radiation absorbed by surfaces and directly controls the distribution of the solar radiation between the surface and the atmosphere. It can significantly impact climate and weather. Betts [56] compared the radiative forcing associated with changes in surface albedo and atmospheric CO_2 and suggested that the positive forcing brought about by forestation-related decreases in albedo in temperate and boreal forest regions could offset the negative forcing expected from carbon sequestration. Dethloff *et al.* [57] found that the changed Arctic sea-ice and snow albedo can trigger changes in the Arctic and North Atlantic Oscillation pattern with strong implications for the European climate. Chapin *et al.* [58] synthesized field data from Arctic Alaska, showing that terrestrial changes in summer albedo contribute substantially to recent high-latitude warming trends.

In terrestrial ecological systems, surface albedo controls the radiation absorption and microclimate conditions of soil and plant canopies, which, in turn, affect ecosystem physical, physiological, and biogeochemical processes such as energy balance, evapotranspiration, plant photosynthesis, and respiration [59].

Climate, biogeochemical, hydrological, and weather forecast models require regional surface albedo with an absolute accuracy of 0.02–0.05 for snow-free and snow-covered land. To monitor anticipated changes in land albedo on the global mean radiation budget, decadal-scale trends in continental-mean surface albedo should be measured to an accuracy of 0.01.

Several ground measurement networks for radiation also include albedo measurements, such as SURFRAD, FLUXNET, BSRN, ARM, and so on. These data sets have been used for validating satellite products and numerical simulations, although the sensors are located at different altitudes with different spatial representations. Scale dis-match has always been an issue between a footprint of only a few square meters for the albedo measurements and a coarse grid of remotely sensed data or simulated data.

A. Remote Sensing Techniques

Three types of data have been used for routine mapping of land surface albedos: multiangle and multispectral data from polar-orbiting satellites, and multispectral data from geostationary satellites. Multiangle sensors include MISR [60], [61] and POLDER [62]; multispectral sensors on polar orbiting platforms include MODIS [63], [64], VIIRS [65], [66], EO1 [67], and others [68]. Sensors on geostationary satellites such as Meteosat and MSG have also been used for albedo mapping [69]–[72].

There are two types of algorithms for estimating land surface broadband albedo from satellite observations: physically-based estimation and direct estimation methods. The physically based estimation methods typically include three steps [68], [73]: (1) atmospheric correction, (2) surface directional reflectance modeling, and (3) narrowband-to-broadband conversion. The first step converts TOA reflectance into surface directional reflectance, the second step converts directional reflectance into spectral albedos, and the last step converts spectral albedos to broadband albedos.

The typical example of physically-based estimation is the MODIS algorithm [63]. The albedo algorithm from the earlier geostationary Meteosat observations [69], [70], [74], [75] combined the first two steps by assuming one unknown constant aerosol optical depth (AOD) for the whole period of time (daily) and eventually ignored the last step since there is only one band available. The algorithm for the Meteosat Second Generation data [72] is very similar to the MODIS one with three steps and known AOD. In physically-based estimation algorithms, the albedo product depends on the performance of all the procedures that characterize the known processes and it is unknown whether errors associated with each procedure cancel or enhance each other.

Instead of retrieving most of the variables explicitly from remote sensing data, the second type of method for albedo calculation is the direct estimation algorithm, which combines all procedures together in one step through regression analysis aiming only to make a best-estimate broadband albedo. The direct retrieval method primarily consists of two steps [64], [76]. The first step produces a large database of TOA directional reflectance and surface albedo for a variety of surface and atmospheric conditions using radiative transfer model simulations. The second step links the simulated TOA reflectance with surface broadband albedo statistically. This method will be used to produce the albedo product from VIIRS in the future.

B. Numerical Simulations

Land surface albedo in climate models is either prescribed as a parameter dependent on land cover types [77] or simulated as an internal variable based on a simplified radiative transfer scheme. The two-stream canopy radiative transfer model for different vegetation types [78]–[80] is one of the most widely used approaches. This scheme has advanced the albedo calculation in climate models from simple land cover based albedo parameterization or look-up tables to more physically based simulation which enables the models to reproduce albedo changes caused by variation in canopy leaf area index (LAI) and optical properties of canopy elements and soil [59]. Such simplified albedo parameterization schemes cannot physically characterize the dynamics of land surfaces.

Numerous studies have found serious discrepancies in these models compared to satellite products [81]–[84]. Wang *et al.* [84] analyzed 17 GCMs participating in the IPCC AR4, and found that the climate model results and satellite-derived products differed up to 0.15–0.19 during winter of northern hemisphere high latitudes. A similar conclusion was found for a global land distribution [85].

Based on satellite albedo products, some improvements have been proposed [86]–[90].

IV. Longwave Downward Radiation

Downward longwave radiation F_d^l is vitally important for numerous applications requiring surface radiation and energy balance, including predicting ET, snowmelt, surface temperature, and frost occurrence.

A. Ground Measurements

The networks mentioned in Section II-A such as BSRN, SURFRAD, ARM, and FLUXNET, also obtain longwave radiation measurements.

The accuracy of downward longwave radiation measurements according to BSRN standards was set to 30 Wm^{-2}, but the pyrgeometers used in the BSRN around 1995 for longwave radiation measurements had accuracies of 10 Wm^{-2} [6]. Recent reports indicated that uncertainties associated with operational BSRN measurements during this period are believed to be about ± 5 Wm^{-2} (1.5%).

B. Remote Sensing Estimates

There have been several comprehensive reviews of methods for estimating surface longwave radiation [22], [91], [92]. The downward longwave radiation algorithms include three types. The first is based on empirical functions using satellite-derived meteorological parameters, for example, the near-surface temperatures and water vapor burden. The second type calculates the radiation quantities with radiative transfer models using satellite-derived atmospheric temperature and water vapor profiles. A strong feature of this approach is the validity of the physics. Type three uses satellite-observed radiances directly to avoid propagation of meteorological parameter retrieval errors in the final radiation estimate. It embeds the physical merits of radiative transfer within the parameterization of nonlinear functions of observed radiance.

The first type of algorithms uses more readily available meteorological observations, such as air temperature, humidity, and solar radiation. Although these simpler algorithms may have larger errors relative to the more complex methods, these methods are needed and useful for a variety of applications. Wang and Liang [13] evaluated two widely accepted methods to estimate global atmospheric downward longwave radiation under all-sky conditions using meteorological observations from 1996 to 2007 at 36 globally-distributed sites, operated by the SURFRAD, AmeriFlux, and AsiaFlux projects, and then applied them to 3200 stations globally to estimate decadal variation from 1973 to 2008. Kjaersgaard *et al.* [93] compared 20 simple models relying solely on air temperature or air temperature plus water vapor pressure using long-term observations. The mean bias errors ranged from -23 to $+12$ Wm^{-2} and -18 to $+15$ Wm^{-2} and RMSE from 39 to 45 Wm^{-2} and 30–36 Wm^{-2} at two sites, respectively. Flerchinger *et al.* [94] evaluated the accuracy of 13 algorithms for predicting incident longwave radiation under clear skies, ten cloud correction algorithms, and four algorithms for all-sky conditions using data from 21 sites across North America and China.

For the second type of algorithms, it is straightforward to calculate F_d^l using atmosphere profiles and a radiative transfer model. However, the physical method is prone to errors in the atmosphere profile. F_d^l is dominated by the radiation from a thin atmospheric layer close to the Earth's surface. The contribution from the atmosphere above 500 m from the surface only accounts for 16–20% of total F_d^l [22], and some satellite sensors cannot capture the atmospheric profiles near the surface.

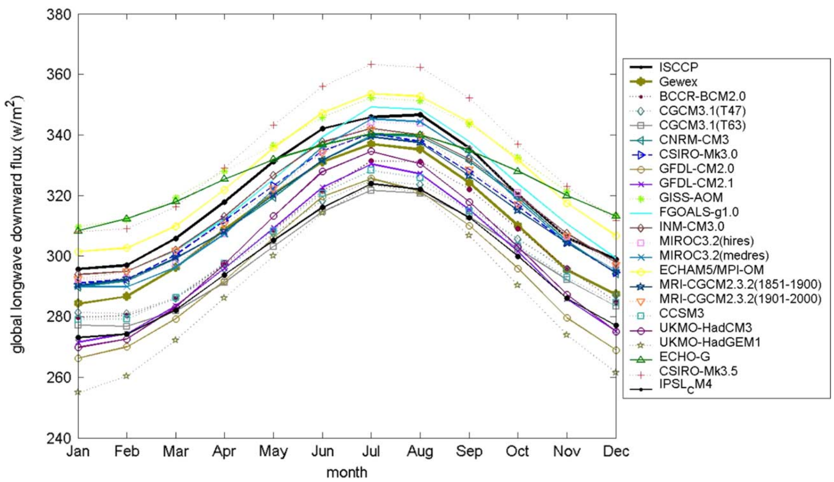

Fig. 1. Monthly averages of longwave downward radiation from two satellite products (ISCCP and GEWEX) and different GCMs in the IPCC AR4.

For example, the vertical resolution of the MODIS-retrieved atmosphere profiles is quite coarse, and only five layers are available between 1000–800 hPa pressure levels; detailed structures of the atmosphere are not captured [95]. Wang and Liang [96] showed that F_d^l is not estimated with acceptable accuracy using the MODIS atmospheric profile product, especially over high altitude surfaces. Most GCMs use this type of algorithm to calculate F_d^l.

The third type of algorithm is often referred to as the hybrid algorithm, which combines physical modeling through radiative transfer simulations and statistical regression that links some of the inputs and output of the simulations [96], [97]. Wang and Liang [96] used the hybrid method to derive clear-sky F_d^l models for MODIS data over land surfaces with the emissivity effect explicitly considered in the radiative transfer simulation process. The validation results show that the derived product has a RMSE of 17.60 Wm^{-2} (Terra) and 16.17 Wm^{-2} (Aqua). A similar algorithm has been developed to estimate clear-sky longwave downward radiation from GOES data [98].

The longwave downward radiation products from remote sensing data include ISCCP-FD, GEWEX, and CERES, as discussed in Section II-B. In addition, the EUMETSAT CM-SAF also produces the monthly longwave downward radiation product by merging AVHRR and SEVERI data [37] with a spatial resolution of 15 km. Based on their official Web site, the GEWEX longwave radiation products have biases of 0.70 (3-hourly), 0.61 (daily) and -2.01 (monthly) Wm^{-2}, and RMS of 31.41 (3-hourly), 22.86 (daily) and 13.63 (monthly) Wm^{-2}.

C. GCM Simulations

All GCMs mentioned in Section II-C can produce longwave downward radiation. Opposite to insolation, the underestimation of downward longwave models is another long standing problem in GCMs [39], [99], [100].

Studies on validating GCM downward longwave radiation are limited. Morcrette [101] validated the ECMWF forecast system used for the ECMWF-40 reanalysis with surface radiation measurements for the April–May 1999 period, available as part of the BSRN, SURFRAD, and ARM programs, and found that the model underestimated observed values by 10 Wm^{-2} or less.

Markovic *et al.* [102] validated the downward longwave radiation of three regional climate models over North America using SURFRAD measurements, and found that for all models all-sky biases are significantly influenced by cloud-free radiation, cloud emissivity and cloud cover errors, with a systematic negative bias during cold, dry conditions, probably due to a combination of omission of trace gas contributions to the downward longwave radiation and a poor treatment of the water vapor continuum at low water vapor concentrations.

Bodas-Salcedo *et al.* [41] found the simulation of downward longwave radiation from the HadGEM1 is closer to observations than its shortwave counterpart with results about 6.0 Wm^{-2} less than the BSRN measurements.

Wild [39] compared the downward longwave radiation of the IPCC AR4 and AMIP II GCMs with measurements at 44 BSRN sites and found that the multiple model mean bias in the IPCC AR4 models amounts to -5.6 Wm^{-2}, which is slightly smaller than in AMIP II $(-8\ \mathrm{Wm}^{-2})$. Improvements in the parameterization of the water vapor continuum can help to remove some of the negative biases in the downward longwave component [103], [104]. The monthly averages of IPCC AR4 models are shown in Fig. 1 which illustrates the significant differences among these GCMs.

Table II shows the average estimates of downward longwave radiation over land surfaces from several sources similar to Table I. The last column value is calculated in this study. It is clear that different estimates of longwave downward radiation from various models and satellite data vary significantly.

D. Decadal Variations

Consistent with global warming, F_d^l increases substantially. Prata [105] calculated using radiative transfer that during the period between 1964 and 1990, there was a global increase in the clear-sky longwave radiation at the Earth's surface. The global trend is approximately $+1.7$ Wm^{-2} per decade. Wang and Liang [13] calculated that, based on 3200 observation stations globally, daily F_d^l increased at an average of 2.2 Wm^{-2} from 1973 to 2008 under all-sky conditions. Wild *et al.* [55] estimated an increase in F_d^l of 2.1 $\mathrm{Wm}^{-2}/\mathrm{decade}$ over the period 1986–2000, and of 2.6 $\mathrm{Wm}^{-2}/\mathrm{decade}$ over the period

TABLE II
ESTIMATED AVERAGE DOWNWARD LONGWAVE RADIATION OVER LAND SURFACES (Wm^{-2})

dataset	ISCCP-FD [163]	NRA [163]	ERA-40 [163]	JRA [163]	Trenberth et al. [163]	IPCC AR4 GCM mean	GEWEX
Feb. 1985-April 1989	318.7	295.9	304.9	286.7		304	309.7
Mar 2000 – May 2004	327.6	296.8		287.4	303.6		

1992–2000 based on BSRN data. The rising trend results from increases in air temperature, atmospheric water vapor and $\mathrm{CO_2}$ concentration. From 1973 to 2008, F_d^l increased worldwide, while high latitudes in the Northern Hemisphere increased at a greater rate.

V. LONGWAVE UPWELLING RADIATION

Longwave upwelling radiation that is highly heterogeneous is very difficult to measure, and point measurements on the ground represent a very small area. As mentioned in Section III-A, multiple surface measurement networks include the measurements of longwave upwelling radiation but they are lacking quantified accuracies. In the following, we briefly review the remote sensing methods and evaluate the GCM simulation results.

A. Remote Sensing Estimates

The upwelling longwave radiation emitted in the spectral wavelengths greater than 4 μ is often referred to as "infrared radiation" or longwave radiation. Given surface skin temperature (T_s) and spectral emissivities (ε_i) that are converted to broadband emissivity (ε) [106]–[108], we can easily calculate this quantity:

$$F_u^l = F_d^l(1-\varepsilon) + \sigma\varepsilon T_s^4 \quad (5)$$

For two-thermal-band sensors, such as AVHRR and GOES, a known emissivity is assumed (or inferred from land cover maps or vegetation indices) to estimate surface skin temperature using a split-window algorithm [68]. Fortunately, the new generation of sensors, such as the Advanced Spaceborne Thermal Emission and Reflection Radiometer (ASTER) and MODIS, has multiple thermal bands that allow the estimation of spectral emissivities and land surface skin temperature simultaneously [109], [110]. Besides MODIS and ASTER, surface skin temperature and emissivity can also be estimated from other satellite sensors [111], such as TM, SEVIRI, AVHRR, ATSR, AATSR, GOES, GMS, VIIRS, and AIRS.

The current surface temperature and emissivity products from remote sensing data still have large uncertainties [112]–[114]. New algorithms for estimating surface emissivity from hyperspectral data [115] or temperature from microwave data [116] deserve further exploration. The alternative solution is to estimate surface longwave upwelling radiation from TOA longwave observations directly. Wang *et al.* [117] applied the hybrid method to estimate upwelling radiation from MODIS using both artificial neural network (ANN) and linear regression, and also compared with the temperature-emissivity based method. They found that the averaged RMSEs of the ANN model method are 15.89 Wm^{-2} (for Terra) and 14.57 Wm^{-2} (for Aqua), and the averaged biases are -8.67 Wm^{-2} (for Terra) and -7.21 Wm^{-2} (for Aqua). The biases and RMSEs of the ANN model method are ~ 5 Wm^{-2} smaller than the temperature-emissivity method and ~ 2.5 Wm^{-2} smaller than the linear regression method.

The longwave upwelling radiation products from remote sensing data include ISCCP-FD, GEWEX, CERES, and EUMETSAT CM-SAF. The monthly averages of two satellite estimates from ISCCP and GEWEX are shown in Fig. 2, and their temporal differences are significant although their annual average values are close.

B. GCM Simulations

Like downward longwave radiation, upwelling longwave radiation simulations from different GCM models have very large differences. Zhang *et al.* [118] found that the difference of skin temperature among four reanalysis data sets is around 2–4°K that can easily cause 10–15 Wm^{-2} uncertainty in calculated surface upwelling longwave fluxes. Most models have simplified surface emissivity, which is another major source of uncertainty [106].

Table III shows the estimates of global upwelling longwave radiation over land surfaces from multiple sources. The last two estimates are obtained in this study. Fig. 2 also compares the monthly averages of upwelling radiation from various IPCC AR4 GCMs. Both Fig. 2 and Table III show significant differences among all these models and satellite estimations.

VI. NET RADIATION

As indicated in (2), all-wave net radiation is the sum of shortwave and longwave net radiation, but the former is much larger than the latter in the day time. Shortwave net radiation depends on both insolation and shortwave albedo. Table I has already shown the significant differences of insolation among GCMs and different satellite estimates, but the differences in albedo are also significant. Wang *et al.* [84] compared IPCC AR4 GCM surface albedo with satellite estimates in the high latitudes. Fig. 3 shows the monthly averages of IPCC AR4 GCMs and three satellite estimates (ISCCP, GEWEX and

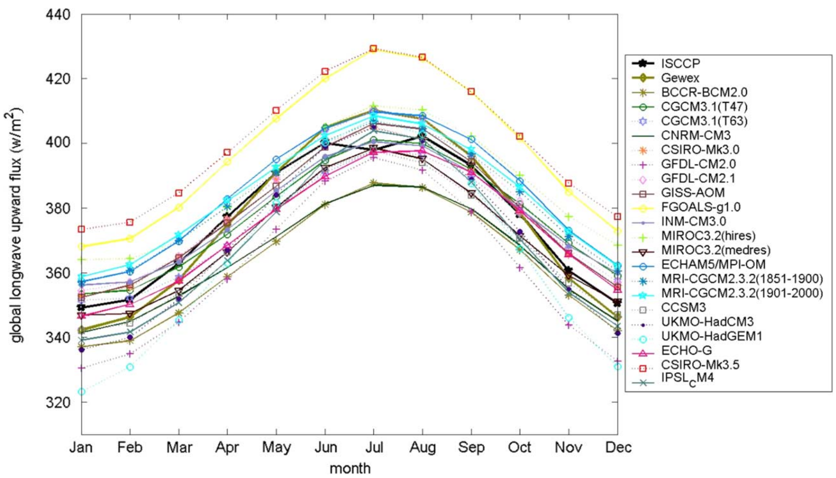

Fig. 2. Monthly averages of longwave upwelling radiation from two satellite products (ISCCP and GEWEX) and different GCMs in the IPCC AR4.

TABLE III
ESTIMATED AVERAGE UPWELLING LONGWAVE RADIATION OVER LAND SURFACES (Wm^{-2})

dataset	ISCCP-FD{ Trenberth, 2009 #2514}	NRA [163]	ERA-40 [163]	JRA [163]	Trenberth et al. [163]	GEWEX	IPCC AR4 GCM mean
Feb. 1985-April 1989	377.8	369.7	370.3	372.7		376.1	372.0
Mar 2000 – May 2004	381.2	371.0		374.4	383.2		

TABLE IV
ESTIMATED AVERAGE SHORTWAVE NET RADIATION OVER LAND SURFACES (Wm^{-2})

dataset	ISCCP-FD [163]	NRA [163]	ERA-40 [163]	JRA [163]	Trenberth et al. [163]	IPCC AR4 GCM mean	GEWEX
Feb. 1985-April 1989	147.2	155.2	134.3	154.9		144.0	140.9
Mar 2000 – May 2004	148.7	155.1		155.8	145.1		

*mean value at 760 stations.

MODIS) over global land surfaces. The global annual mean land albedo varies from 0.18–0.26 [85].

Table IV shows the average estimates of shortwave net radiation from various sources. We calculated the values in the last two columns.

As shown in (4), longwave net radiation is the difference between downward and upwelling radiation. There are multiple error sources [119], a significant difficulty in the estimation of the incident longwave flux at the surface is quantifying the effects of clouds [92]. As Diak *et al.* [120] pointed out, a satellite monitors the temperature of the cloud top, however, the cloud-base temperature is a critical quantity controlling the downward longwave radiation at the surface under cloudy conditions. The common practice is to correct the cloud effect using cloud information [13], [121], [122]. For example, Diak [123] provided a parameterization of downward longwave radiation under cloudy skies from GOES data using cloud temperature and emissivity, and Flerchinger *et al.* [94] compared eight models based on cloud coverage and two models based on solar index. We developed a method to estimate net radiation under both clear-sky and cloudy conditions from solar radiation, which is validated to accurately predict long-term variation in net radiation [124].

As discussed in Sections II-C and IV-C, most GCMs overestimate insolation but underestimate longwave downward radiation, however, the overall net radiation remains more or less correct globally [39], while this cancellation no longer applies on regional, seasonal, and diurnal time scales.

VII. Evapotranspiration

Evapotranspiration (ET) is a major component of the terrestrial water, energy, and biogeochemical cycles. It is the sum of water lost to the atmosphere from the soil surface through evaporation and from plant tissues via transpiration, and cools the surface and moistens the atmosphere near the Earth's surface. Hence, characterizing its regional and global variability and change is important.

The most accurate measurements of ET have been made locally. ET is not readily observable with remote sensing, but can be calculated (inferred) from some products generated from remote sensing data. Different land surface models yield different ET values even when the same forcing data are used.

A. Ground Measurements

ET from land surfaces has not been well observed with *in situ* instruments. Micrometeorological based methods are widely employed [125], [126], such as Bowen ratio energy balance (BREB), and eddy covariance (EC). Weighing lysimeters have also been commonly applied to measure the ET at ground level, and provide the only direct measure of water flux from a vegetated surface.

The BREB method uses direct measurements of net radiation $(\mathrm{R_n})$, ground flux (G), and gradients of temperature and water vapor in the atmosphere to estimate latent heat flux (ET) and sensible heat flux (H) by assuming similarity between heat and water vapor transport and conservation of energy. It is independent of weather conditions and requires no information about aerodynamic characteristics of the experimental surface. However, any inaccuracy in one of the instruments will reflect directly on all heat fluxes.

The EC method is based on direct measurements of the product of vertical velocity fluctuations and scalar concentration fluctuations yielding a direct estimate of H and LE assuming the mean vertical velocity is negligible. The EC method has overtaken the BREB as being the preferred micrometeorological technique for ET measurement because it involves minimal theoretical assumptions and is now affordable and available off-the-shelf. However, it suffers from an energy imbalance problem. Clearly the BREB method must be consistent with conservation of energy because it forces energy-balance closure; however, the EC method provides estimates of H and LE separately so that when combined with measurements of Rn, G, and S all major components of the energy balance are independently measured. An average imbalance of 20% across 22 FLUXNET eddy correlation sites was attributed to underestimated $(H + \mathrm{ET})$ and/or overestimated available energy [127]. A 10% to 30% underestimation of $(H + \mathrm{ET})$ was reported even over relatively flat homogenous short vegetation [128], and the closure error is typically higher over strongly evaporating surfaces such as irrigated crops.

The common belief is that measuring errors or storage terms are the reason for the unclosed energy balance, however, Foken [129] argued that exchange processes on larger scales of the heterogeneous landscape have a significant influence and the problem is actually a scale problem.

BREB and EC use *in situ* observations that can provide direct, site-specific estimates of ET at high temporal resolution. However, spatial heterogeneity and the relatively few number of sites prevent direct scaling of these calculations to regional estimates. Regional measurements can be made through airborne measurement systems [130] at short temporal scales, but the cost is prohibitive for wide use. One alternative solution is the development of a mobile system [131]. In recent years progress has been made in making theory-based area-average estimates of evaporation using scintillometers. For example, Kleissl *et al.* [132] reported a first-of-its-kind network of seven large aperture scintillometer (LAS) sites in New Mexico established in 2006 to measure sensible heat fluxes over irrigated fields, riparian areas, deserts, lava flows, and mountain highlands.

B. Remote Sensing Estimates

Despite the inability to measure ET directly with remote sensing, it is possible to measure states and processes that are needed to estimate ET. Various remote sensing techniques have been used to estimate ET at different scales [133]–[136]. Unfortunately, none of these methods estimate ET very accurately, with an average RMSE value for all of about 50 $\mathrm{Wm^{-2}}$ and relative errors of 15–30%. We briefly introduce three methods: statistical methods, energy balance based methods, and data assimilation methods.

In natural ecosystems the vegetation indexes may be used for up-scaling from ground based ET? measurements from flux towers to larger spatial domains. For example, Nagler *et al.* [137] correlated 16-day MODIS EVI values with ET observations obtained with flux towers in semi-arid rangeland in Arizona, and a simple multiple linear regression fit of ET to EVI resulted in the correlation coefficient of 0.80–0.94. To use both vegetation index and thermal brightness temperature, the so-called "triangle method" has also been used for estimating ET fraction, which is the ratio of the ET and available energy (net radiation) [138]. This method is named this way because the scatters of the pixels in the two-dimensional space of temperature and vegetation indexes form a triangle shape. To incorporate the surface moisture status, Wang and Liang [4] developed a statistical formula using ground measurements over the US Southern Great Plains based on vegetation index, air or surface skin temperature and their day/night difference. A similar approach was also explored by Yang *et al.* [139] who used the support vector machines, a widely used machine learning technique.

Building on recent advances in ecophysiological theory that allows detection of multiple stresses on plant function using biophysical remote sensing metrics, some formulae for calculating potential ET have been extended to calculate the actual ET globally but by using both meteorological observations and remote sensing products, for example, the Priestley-Taylor Formula [140] and the Penman-Monteith (PM) formula [141], [142]. The revised PM algorithm [141] can estimate the 8-day latent heat flux (LE) from the MODIS data with a RMSE of 27.3 $\mathrm{Wm^{-2}}$ using tower meteorological data, and 29.5 $\mathrm{Wm^{-2}}$ with reanalysis data.

TABLE V
ESTIMATED AVERAGE LATENT HEAT FLUX FROM ET OVER LAND SURFACES (Wm^{-2})

dataset	NRA [163]	ERA-40 [163]	JRA [163]	Trenberth et al. [163]	NCEP-2	IPCC-AR4 model mean	GLDAS	GSWP-2	Yiao et al. [166]
Feb. 1985-April 1989	52.0	40.9	39.5		50.14	42.0	29.99	29.59	29.77
Mar 2000 – May 2004	50.2	-	39.4	38.5					

Many algorithms have been developed to estimate ET based on energy balance [91], [143], [144]. Most of them attempt to calculate ET as a residual of the energy balance equation (e.g., (1)), once R_n, G and H are determined through a combination of ground, remote sensing, and modeling techniques. These models use information available from the scene in remotely sensed imagery to provide context for estimating the surface energy budget components, typically one-source models [145], [146] that treat the landscape as a single unit; and two source models [143], [147] that divide the landscape into vegetated and non-vegetated units, and estimate the surface energy budget for each separately.

Given the inability to accurately measure ET directly over large areas with *in situ* or remote sensing methods, assimilating remotely sensed products into land surface models that have improved boundary-layer physics for estimating ET is another active research area and the most important progress may likely be made in this area [148], [149].

ET is also a component of the water budget:

$$dS/dt = P - ET - Q \tag{6}$$

where S is land water storage (e.g., snow, soil moisture, lakes/reservoirs/streams, canopy storage), P is precipitation, and Q is runoff/streamflow. All these water budget components can now be estimated from remote sensing data [150]–[152], for example, changes in total surface and subsurface storage dS/dt can be derived using gravity anomaly measurements, such as the Gravity Recovery and Climate Experiment (GRACE) launched in March 2002 [153], [154], P is regularly retrieved using a variety of techniques from multi-sensor microwave and infrared data, such as the Tropical Rainfall Measuring Mission (TRMM) satellite [155] and the Climate Prediction Center morphing method (CMORPH) [156], and Q from laser altimetry and interferometric synthetic aperture radiometry technologies data [157]. Thus, ET can also be estimated from the water budget equation in principle at regional and continental scales, but there are currently large uncertainties in estimating the individual components [151]. With the Surface Water Ocean Topography (SWOT) mission in the near future, all components of the water budget can be well observed.

C. Model Simulations

Almost all atmospheric GCM models have a land surface energy balance module [144] for simulating the individual heat fluxes. The modeling development has been recently reviewed by Shuttleworth [158]. Current model simulations do not provide the degree of accuracy required for climate and weather prediction. For example, even when forced by the same dataset, land surface models from the North American Land Data Assimilation System differ substantially from each other in ET simulation [159], although their parameterizations appear to be similar in some ways.

Different model simulations vary significantly and ET climatology is not well known [160], [161]. For example, Grotjahn [162] pointed out that the surface energy budgets differ between the ECMWF ERA-40 and NCEP NDRa2 reanalysis datasets in that ERA-40 data have greater sensible heat flux into the air, while NDRa2 data have greater latent heat flux.

Table V shows the global average latent heat flux from ET over land surfaces. The first four estimates were given by Trenberth *et al.* [163], and the last five numbers are estimated in this study, where both Global Soil Wetness Project 2 (GSWP-2) [164], [165] and the Global Land Data Assimilation System (GLDAS) ET estimates are averages of model simulations. The last number is based on the statistical formula developed by Yao *et al.* [166]. It is clear that the differences of various estimates are also very significant.

D. Temporal Variations

One expected consequence of global warming is the increase in ET. Long-term data records have been maintained for the evaporative loss from a pan of water. Numerous studies [167], [168] have reported decreasing pan evaporation over large areas and in different regions of the world over the past 50 years. These decreases in pan evaporation are interpreted to be the result of a number of mechanisms, e.g., decreasing surface solar radiation [169] and decreasing wind speed [170]. The contrast between the expected and observed ET is called the "evaporation paradox".

Cong *et al.* [171] found that from 1956 to 2005, the pan evaporation paradox existed in China as a whole while pan evaporation kept decreasing and air temperature became warmer and warmer, but the actual evaporation decreased in the former 30 years and increased in the latter 20 year for the whole of China. Gordon *et al.* [172] found that ET decreased in southeastern China, the eastern U.S. and the U.K. over the past 30 years, but has increased in the western U.S. and northwestern China. Other water budget-based studies showed long-term changes in ET in northeastern and middle China [4], [173], decreases over the eastern U.S., and increases over the western U.S. [174]–[176]. Teuling *et al.* [177] demonstrated the strong regional and temporal differentiation of trends in actual evaporation. Using a modified Penman-Monteith method with station measurements, Wang *et al.* [3] recently calculated that the ET daytime value increased by 0.18 Wm^{-2} $year^{-1}$ averaged over all 858 stations, or 3.7 Wm^{-2} (4% in relative value) from 1982 to 2002, equal to 24 mm $year^{-1}$ in water flux, and increased solar radiation and vegetation cover (quantified by vegetation index) are the two most important factors determining the long-term increase in ET.

VIII. Conclusion

We have reviewed the recent advances in estimating land surface radiation and energy budget components from ground measurements, remote sensing techniques and numerical simulations. Though progress has been made, the task still faces many challenges.

Differences between various numerical model simulations are quite significant, which may be the result of different model physics, model structure, and input/forcing data. Compared to ground measurements, most state-of-the-art GCMs still tend to overestimate the surface incident shortwave radiation, which has been a long standing problem. The overestimation in some reanalysis data sets is even much larger. Concerning land surface albedo, most GCMs tend to underestimate this parameter compared to estimates from MODIS. Opposite to incident shortwave radiation, the underestimation of downward longwave models is another long standing problem in GCMs. Fortunately, GCMs simulate the net radiation reasonably well globally due to overestimation of insolation and underestimation of downward longwave radiation. The cancellation of errors is probably a consequence of the energy conservation implemented in the models. Because of the uncertainties, the simulation results do not well characterize the decadal variations in land surface radiation and energy budgets.

Remotely sensed products are usually considered to be the most appropriate sources to verify and test the accuracy of numerical models, but most of the surface radiation and energy budget components have to be estimated from satellite observations, and the inversion process always introduces uncertainties. However, as the inversion algorithms approach maturity, the uncertainties of satellite products are becoming smaller than those in the numerical model simulations and the satellite products will be used more and more effectively for model initialization, calibration and validation.

The retrieved remotely sensed quantities have to be validated by ground measurements. The ground "point" measurements cannot match the size of the remote sensing pixel or model grid spatially. Spatial upscaling always results in errors, but the use of remote sensing observations with different spatial resolutions will help to reduce uncertainties. Overall, the number of current ground measurement networks is inadequate for a good spatial and temporal representation. Uncertainties of ground measurements in different networks, or even in the same network, vary considerably, and cross-calibration is highly needed. Consistent processing and effective management of ground measurements from various sources to make them accessible to the users remains a considerable challenge.

The ultimate solution may be to assimilate all observations and data products from various sources into the numerical models to generate accurate spatiotemporal continuous land surface radiation and energy budgets. It is becoming an active research area.

One difficult issue we were faced with is the variable error measures used by different studies, such as the bias, RMSE, RMS, percentage error, STD, and so on. This makes intercomparisons of the errors among ground measurements, satellite products and numerical simulations difficult. One point is that the comparison with ground based measurements does not adequately provide the error of the model or inversion algorithm. Even a perfect model or retrieval algorithm would fail if it is feed with inaccurate input data.

Acknowledgment

This paper benefits from the presentations and discussions of the International Conference on Land Surface Radiation and Energy Budgets, March 18–20, 2009, Beijing, China. The authors would like to thank reviewers for their valuable comments and suggestions, and Dr. Carol Russell for editing the paper.

References

[1] S. W. Running, R. R. Nemani, F. A. Heinsch, M. S. Zhao, M. Reeves, and H. Hashimoto, "A continuous satellite-derived measure of global terrestrial primary production," *BioScience*, vol. 54, pp. 547–560, Jun. 2004.

[2] S. D. Prince and S. N. Goward, "Global primary production: A remote sensing approach," *J. Biogeography*, vol. 22, pp. 815–835, 1995.

[3] K. Wang, R. E. Dickinson, M. Wild, and S. Liang, "Evidence for decadal variation in terrestrial evapotranspiration between 1982 and 2002, Results," *J. Geophys. Res.*, 2010.

[4] K. Wang and S. Liang, "An improved method for estimating global evapotranspiration based on satellite determination of surface net radiation, vegetation index, temperature, and soil moisture," *J. Hydrometeorol.*, vol. 9, pp. 712–727, Aug. 2008.

[5] H. Gilgen and A. Ohmura, "The global energy balance archive," *Bull. Amer. Meteorol. Soc.*, vol. 80, pp. 831–850, May 1999.

[6] A. Ohmura, E. G. Dutton, B. Forgan, C. Frohlich, H. Gilgen, H. Hegner, A. Heimo, G. Konig-Langlo, B. McArthur, G. Muller, R. Philipona, R. Pinker, C. H. Whitlock, K. Dehne, and M. Wild, "Baseline Surface Radiation Network (BSRN/WCRP): New precision radiometry for climate research," *Bull. Amer. Meteorol. Soc.*, vol. 79, pp. 2115–2136, Oct. 1998.

[7] J. A. Augustine, J. J. DeLuisi, and C. N. Long, "SURFRAD—A national surface radiation budget network for atmospheric research," *Bull. Amer. Meteorol. Soc.*, vol. 81, pp. 2341–2357, Oct. 2000.

[8] J. A. Augustine, G. B. Hodges, C. R. Cornwall, J. J. Michalsky, and C. I. Medina, "An update on SURFRAD—The GCOS Surface Radiation budget network for the continental United States," *J. Atmospher. Ocean. Technol.*, vol. 22, pp. 1460–1472, Oct. 2005.

[9] D. Baldocchi, E. Falge, L. H. Gu, R. Olson, D. Hollinger, S. Running, P. Anthoni, C. Bernhofer, K. Davis, R. Evans, J. Fuentes, A. Goldstein, G. Katul, B. Law, X. H. Lee, Y. Malhi, T. Meyers, W. Munger, W. Oechel, K. Pilegaard, H. P. Schmid, R. Valentini, S. Verma, T. Vesala, K. Wilson, and S. Wofsy, "FLUXNET: A new tool to study the temporal and spatial variability of ecosystem-scale carbon dioxide, water vapor, and energy flux densities," *Bull. Amer. Meteorol. Soc.*, vol. 82, pp. 2415–2434, 2001.

[10] H. Gilgen, M. Wild, and A. Ohmura, "Means and trends of shortwave incoming radiation at the surface estimated from Global Energy Balance Archive data," *J. Climate*, vol. 11, pp. 2042–2061, 1998.

[11] K. Yang, R. T. Pinker, Y. Ma, T. Koike, M. M. Wonsick, S. J. Cox, Y. Zhang, and P. Stackhouse, "Evaluation of satellite estimates of downward shortwave radiation over the Tibetan Plateau," *J. Geophys. Res. –Atmospheres*, vol. 113, p. 11, Sep. 2008.

[12] O. E. Garcia, A. M. Diaz, F. J. Exposito, J. P. Diaz, O. Dubovik, P. Dubuisson, J. C. Roger, T. F. Eck, A. Sinyuk, Y. Derimian, E. G. Dutton, J. S. Schafer, B. N. Holben, and C. A. Garcia, "Validation of AERONET estimates of atmospheric solar fluxes and aerosol radiative forcing by ground-based broadband measurements," *J. Geophys. Res.–Atmospheres*, vol. 113, p. 16, Nov. 2008.

[13] K. Wang and S. Liang, "Global atmospheric downward longwave radiation over land surface under all-sky conditions from 1973 to 2008," *J. Geophys. Res.–Atmospheres*, vol. 114, 2009, 10.1029/2009JD011800.

[14] H. Jacobowitz and R. J. Tighe *et al.*, "The Earth radiation budget derived from the Nimbus-7 ERB experiment," *J. Geophys. Res.*, vol. 89, pp. 4997–5010, 1984.

[15] B. R. Barkstrom and G. L. Smith, "The earth radiation budget experiment: Science and implementation," *Rev. Geophys.*, vol. 24, pp. 379–390, 1986.

[16] B. A. Wielicki, B. R. Barkstrom, B. A. Baum, T. P. Charlock, R. N. Green, D. P. Kratz, R. B. I. Lee, P. Minnis, G. L. Smith, T. Wong, D. F. Young, R. D. Cess, J. A. J. Coakley, D. A. Crommelynck, L. Donner, R. Kandel, M. D. King, A. J. Miller, V. Ramanathan, D. A. Randall, L. L. Stowe, and R. M. Welch, "Clouds and the Earth's Radiant Energy System (CERES): Algorithm overview," *IEEE Trans. Geosci. Remote Sens.*, vol. 36, pp. 1127–1141, 1998.

[17] J. E. Harries, J. E. Russell, J. A. Hanafin, H. Brindley, J. Futyan, J. Rufus, S. Kellock, G. Matthews, R. Wrigley, A. Last, J. Mueller, R. Mossavati, J. Ashmall, E. Sawyer, D. Parker, M. Caldwell, P. M. Allan, A. Smith, M. J. Bates, B. Coan, B. C. Stewart, D. R. Lepine, L. A. Cornwall, D. R. Corney, M. J. Ricketts, D. Drummond, D. Smart, R. Cutler, S. Dewitte, N. Clerbaux, L. Gonzalez, A. Ipe, C. Bertrand, A. Joukoff, D. Crommelynck, N. Nelms, D. T. Llewellyn-Jones, G. Butcher, G. L. Smith, Z. P. Szewczyk, P. E. Mlynczak, A. Slingo, R. P. Allan, and M. A. Ringer, "The geostationary Earth Radiation Budget Project," *Bull. Amer. Meteorol. Soc.*, vol. 86, pp. 945–960, Jul. 2005.

[18] J. Schmetz, P. Pili, S. Tjemkes, D. Just, J. Kerkmann, S. Rota, and A. Ratier, "An introduction to Meteosat Second Generation (MSG)," *Bull. Amer. Meteorol. Soc.*, vol. 83, p. 977, Jul. 2002.

[19] R. T. Pinker, X. Li, W. Meng, and E. A. Yegorova, "Toward improved satellite estimates of short-wave radiative fluxes—Focus on cloud detection over snow: 2. Results," *J. Geophys. Res.–Atmospheres*, vol. 112, May 2007.

[20] I. Laszlo, P. Ciren, H. Q. Liu, S. Kondragunta, J. D. Tarpley, and M. D. Goldberg, "Remote sensing of aerosol and radiation from geostationary satellites," *Adv. Space Res.*, vol. 41, pp. 1882–1893, 2008.

[21] S. Liang, T. Zheng, R. Liu, H. Fang, S. C. Tsay, and S. Running, "Mapping incident Photosynthetically Active Radiation (PAR) from MODIS Data," *J. Geophys. Res.–Atmospheres*, vol. 111, 2006, 10.1029/2005JD006730, Art. No. D15208.

[22] J. Schmetz, "Towards a surface radiation climatology: Retrieval of downward irradiances from satellites," *Atmospher. Res.*, vol. 23, pp. 287–321, 1989.

[23] R. T. Pinker, R. Frouin, and Z. Li, "A review of satellite methods to derive surface shortwave irradiance," *Remote Sens. Environ.*, vol. 51, pp. 108–124, 1995.

[24] S. Gui, S. Liang, K. Wang, and L. Li, "Validation of three satellite-estimated land surface downward shortwave radiation datasets," *IEEE Geosci. Remote Sens. Lett.*, 2010, in press.

[25] C. Whitlock, T. Charlock, W. Staylor, R. Pinker, I. Laszlo, A. Ohmura, G. H. , T. Konzelman, R. C. DiPasquale, C. D. Moats, S. R. LeCroy, and N. A. Ritchey, "First global WCRP shortwave surface radiation budget dataset," *Bull. Amer. Meteorol. Soc.*, vol. 76, pp. 905–922, 1995.

[26] Y. C. Zhang, W. B. Rossow, A. A. Lacis, V. Oinas, and M. I. Mishchenko, "Calculation of radiative fluxes from the surface to top of atmosphere based on ISCCP and other global data sets: Refinements of the radiative transfer model and the input data," *J. Geophys. Res.–Atmospheres*, vol. 109, Oct. 6, 2004, Art. No. D19105.

[27] E. Raschke, S. Bakan, and S. Kinne, "An assessment of radiation budget data provided by the ISCCP and GEWEX-SRB," *Geophys. Res. Lett.*, vol. 33, Apr. 12, 2006.

[28] H. M. Deneke, A. J. Feijt, and R. A. Roebeling, "Estimating surface solar irradiance from METEOSAT SEVIRI-derived cloud properties," *Remote Sens. Environ.*, vol. 112, pp. 3131–3141, Jun. 2008.

[29] Z. Li and H. G. Leighton, "Global climatology of solar radiation budgets at the surface and in the atmosphere from 5 years of ERBE data," *J. Geophys. Res.*, vol. 98, 1993.

[30] Z. Li, H. G. Leighton, K. Masuda, and T. Takashima, "Estimation of SW flux absorbed at the surface from TOA reflected flux," *J. Climate*, vol. 6, pp. 317–330, 1993.

[31] R. Liu, S. Liang, H. He, J. Liu, and T. Zheng, "Mapping photosynthetically active radiation from MODIS data in China," *Remote Sens. Environ.*, vol. 112, pp. 998–1009, 2008.

[32] T. Zheng, S. Liang, and K. C. Wang, "Estimation of incident PAR from GOES imagery," *J. Appl. Meteorol. Climatol.*, vol. 47, pp. 853–868, 2008.

[33] S. Liang, T. Zheng, D. D. Wang, K. C. Wang, R. G. Liu, S. C. Tsay, S. Running, and J. Townshend, "Mapping high-resolution incident photosynthetically active radiation over land from polar-orbiting and geostationary satellite data," *Photogramm. Eng. Remote Sens.*, vol. 73, pp. 1085–1089, Oct. 2007.

[34] R. T. Pinker, J. D. Tarpley, I. Laszlo, K. E. Mitchell, P. R. Houser, E. F. Wood, J. C. Schaake, A. Robock, D. Lohmann, B. A. Cosgrove, J. Sheffield, Q. Y. Duan, L. F. Luo, and R. W. Higgins, "Surface radiation budgets in support of the GEWEX Continental-Scale International Project (GCIP) and the GEWEX Americas Prediction Project (GAPP), including the North American Land Data Assimilation System (NLDAS) Project," *J. Geophys. Res.*, vol. 108, Nov. 19, 2003, Art. N. 8844.

[35] G. R. Diak and C. Gautier, "Improvements to a simple physical model for estimating insolation from GOES data," *J. Climate Appl. Meteorol.*, vol. 22, pp. 505–508, 1983.

[36] J. A. Otkin, M. C. Anderson, J. R. Mecikalski, and G. R. Diak, "Validation of GOES-based insolation estimates using data from the US Climate Reference Network," *J. Hydrometeorol.*, vol. 6, pp. 460–475, Aug. 2005.

[37] J. Schulz, P. Albert, H. D. Behr, D. Caprion, H. Deneke, S. Dewitte, B. Durr, P. Fuchs, A. Gratzki, P. Hechler, R. Hollmann, S. Johnston, K. G. Karlsson, T. Manninen, R. Muller, M. Reuter, A. Riihela, R. Roebeling, N. Selbach, A. Tetzlaff, W. Thomas, M. Werscheck, E. Wolters, and A. Zelenka, "Operational climate monitoring from space: The EUMETSAT Satellite Application Facility on Climate Monitoring (CM-SAF)," *Atmospher. Chem. Phys.*, vol. 9, pp. 1687–1709, 2009.

[38] R. W. Mueller, C. Matsoukas, A. Gratzki, H. D. Behr, and R. Hollmann, "The CM-SAF operational scheme for the satellite based retrieval of solar surface irradiance—A LUT based eigenvector hybrid approach," *Remote Sens. Environ.*, vol. 113, pp. 1012–1024, May 2009.

[39] M. Wild, "Short-wave and long-wave surface radiation budgets in GCMs: A review based on the IPCC-AR4/CMIP3 models," *Tellus Series a–Dynamic Meteorology and Oceanography*, vol. 60, pp. 932–945, Oct. 2008.

[40] M. Wild, "How well do IPCC-AR4/CMIP3 climate models simulate global dimming/brightening and twentieth-century daytime and nighttime warming?," *J. Geophys. Res.–Atmospheres*, vol. 114, May 2009.

[41] A. Bodas-Salcedo, M. A. Ringer, and A. Jones, "Evaluation of the surface radiation budget in the atmospheric component of the Hadley Centre Global Environmental Model (HadGEM1)," *J. Climate*, vol. 21, pp. 4723–4748, Sep. 2008.

[42] X. A. Xia, P. C. Wang, H. B. Chen, and F. Liang, "Analysis of downwelling surface solar radiation in China from National Centers for Environmental Prediction reanalysis, satellite estimates, and surface observations," *J. Geophys. Res.–Atmospheres*, vol. 111, p. 9, May 2006.

[43] F. Babst, R. W. Mueller, and R. Hollmarm, "Verification of NCEP reanalysis shortwave radiation with mesoscale remote sensing data," *IEEE Geosci. Remote Sens. Lett.*, vol. 5, pp. 34–37, Jan. 2008.

[44] M. Zhao, S. Running, and R. Nemani, "Sensitivity of Moderate Resolution Imaging Spectroradiometer (MODIS) terrestrial primary production to the accuracy of meteorological reanalyses," *J. Geophys. Res.*, vol. 111, p. G01002, 2006, 10.1029/2004JG000004.

[45] A. Ohmura, "Observed decadal variations in surface solar radiation and their causes," *J. Geophys. Res.–Atmospheres*, vol. 114, Apr. 2009.

[46] M. Wild, H. Gilgen, A. Roesch, A. Ohmura, C. N. Long, E. G. Dutton, B. Forgan, A. Kallis, V. Russak, and A. Tsvetkov, "From dimming to brightening: Decadal changes in solar radiation at Earth's surface," *Science*, vol. 308, pp. 847–850, May 6, 2005.

[47] M. Wild, B. Truessel, A. Ohmura, C. N. Long, G. Konig-Langlo, E. G. Dutton, and A. Tsvetkov, "Global dimming and brightening: An update beyond 2000," *J. Geophys. Res.–Atmospheres*, vol. 114, p. 14, May 2009.

[48] V. Ramanathan and Y. Feng, "Air pollution, greenhouse gases and climate change: Global and regional perspectives," *Atmospher. Environ.*, vol. 43, pp. 37–50, Jan. 2009.

[49] A. T. Evan, A. K. Heidinger, and D. J. Vimont, "Arguments against a physical long-term trend in global ISCCP cloud amounts," *Geophys. Res. Lett.*, vol. 34, p. 5, Feb. 2007.

[50] T. Hayasaka, K. Kawamoto, G. Y. Shi, and A. Ohmura, "Importance of aerosols in satellite-derived estimates of surface shortwave irradiance over China," *Geophys. Res. Lett.*, vol. 33, p. 4, Mar. 2006.

[51] K. Makowski, M. Wild, and A. Ohmura, "Diurnal temperature range over Europe between 1950 and 2005," *Atmospher. Chem. Phys.*, vol. 8, pp. 6483–6498, 2008.

[52] K. Makowski, E. B. Jaeger, M. Chiacchio, M. Wild, T. Ewen, and A. Ohmura, "On the relationship between diurnal temperature range and surface solar radiation in Europe," *J. Geophys. Res.–Atmospheres*, vol. 114, p. 16, Apr. 2009.

[53] M. Wild, "Global dimming and brightening: A review," *J. Geophys. Res.–Atmospheres*, vol. 114, p. 31, Jun. 2009.

[54] M. Wild, A. Ohmura, and K. Makowski, "Impact of global dimming and brightening on global warming," *Geophys. Res. Lett.*, vol. 34, p. 4, Feb. 2007.

[55] M. Wild, J. Grieser, and C. Schaer, "Combined surface solar brightening and increasing greenhouse effect support recent intensification of the global land-based hydrological cycle," *Geophys. Res. Lett.*, vol. 35, p. 5, Sep. 2008.

[56] R. A. Betts, "Offset of the potential carbon sink from boreal forestation by decreases in surface albedo," *Nature*, vol. 408, pp. 187–190, Nov. 2000.

[57] K. Dethloff, A. Rinke, A. Benkel, M. Koltzow, E. Sokolova, S. K. Saha, D. Handorf, W. Dorn, B. Rockel, H. von Storch, J. E. Haugen, L. P. Roed, E. Roeckner, J. H. Christensen, and M. Stendel, "A dynamical link between the Arctic and the global climate system," *Geophys. Res. Lett.*, vol. 33, Feb. 1, 2006.

[58] F. S. Chapin, M. Sturm, M. C. Serreze, J. P. McFadden, J. R. Key, A. H. Lloyd, A. D. McGuire, T. S. Rupp, A. H. Lynch, J. P. Schimel, J. Beringer, W. L. Chapman, H. E. Epstein, E. S. Euskirchen, L. D. Hinzman, G. Jia, C. L. Ping, K. D. Tape, C. D. C. Thompson, D. A. Walker, and J. M. Welker, "Role of land-surface changes in Arctic summer warming," *Science*, vol. 310, pp. 657–660, Oct. 2005.

[59] S. Wang, A. P. Trishchenko, and X. M. Sun, "Simulation of canopy radiation transfer and surface albedo in the EALCO model," *Climate Dynamics*, vol. 29, pp. 615–632, Nov. 2007.

[60] J. V. Martonchik, D. J. Diner, B. Pinty, M. M. Verstraete, R. B. Myneni, Y. Knyazikhin, and H. R. Gordon, "Determination of land and ocean reflective, radiative, and biophysical properties using multiangle imaging," *IEEE Trans. Geosci. Remote Sens.*, vol. 36, pp. 1266–1281, 1998.

[61] D. J. Diner, J. V. Martonchik, R. A. Kahn, B. Pinty, N. Gobron, D. L. Nelson, and B. N. Holben, "Using angular and spectral shape similarity constraints to improve MISR aerosol and surface retrievals over land," *Remote Sens. Environ.*, vol. 94, pp. 155–171, Jan. 30, 2005.

[62] M. Leroy, J. L. Deuze, F. M. Breon, O. Hautecoeur, M. Herman, J. C. Buriez, D. Tanre, S. Bouffies, P. Chazette, and J. L. Roujean, "Retrieval of atmospheric properties and surface bidirectional reflectances over land from POLDER/ADEOS," *J. Geophys. Res.*, vol. 102, pp. 17023–17037, 1997.

[63] C. Schaaf, F. Gao, A. Strahler, W. Lucht, X. Li, T. Tsung, N. Strugll, X. Zhang, Y. Jin, P. Muller, P. Lewis, M. Barnsley, P. Hobson, M. Disney, G. Roberts, M. Dunderdale, C. Doll, R. d'Entremont, B. Hu, S. Liang, J. Privette, and D. Roy, "First operational BRDF, albedo nadir reflectance products from MODIS," *Remote Sens. Environ.*, vol. 83, pp. 135–148, 2002.

[64] S. Liang, J. Stroeve, and J. E. Box, "Mapping daily snow/ice shortwave broadband albedo from Moderate Resolution Imaging Spectroradiometer (MODIS): The improved direct retrieval algorithm and validation with Greenland *in situ* measurement," *J. Geophys. Res.–Atmospheres*, vol. 110, May 26, 2005, Art. No. D10109.

[65] S. Miller, Surface Albedo: Visible/Infrared Imager/Radiometer Suite Algorithm Theoretical Basis Document, Version 5 Ratheon Systems Company, SBRS Document # Y2398, 2002.

[66] S. Liang, Y. Yu, and T. P. Defelice, "VIIRS narrowband to broadband land surface albedo conversion: Formula and validation," *Int. J. Remote Sens.*, vol. 26, pp. 1019–1025, Mar. 10, 2005.

[67] S. Liang, H. Fang, M. Kaul, T. G. Van Niel, T. R. McVicar, J. Pearlman, C. L. Walthall, C. Daughtry, and K. F. Huemmrich, "Estimation of land surface broadband albedos and leaf area index from EO-1 ALI data and validation," *IEEE Trans. Geosci. Remote Sens.*, vol. 41, pp. 1260–1268, 2003.

[68] S. Liang, *Quantitative Remote Sensing of Land Surfaces*. New York: John Wiley & Sons, Inc., 2004.

[69] B. Pinty, F. Roveda, M. M. Verstraete, N. Gobron, Y. Govaerts, J. V. Martonchik, D. J. Diner, and R. A. Kahn, "Surface albedo retrieval from Metrosat. I. Theory," *J. Geophys. Res.*, vol. 105, pp. 18099–18112, 2000.

[70] B. Pinty, F. Roveda, M. M. Verstraete, N. Gobron, Y. Govaerts, J. V. Martonchik, D. J. Diner, and R. A. Kahn, "Surface albedo retrieval from Metrosat. II. Applications," *J. Geophys. Res.*, vol. 105, pp. 18113–18134, 2000.

[71] Y. M. Govaerts, A. Lattanzio, M. Taberner, and B. Pinty, "Generating global surface albedo products from multiple geostationary satellites," *Remote Sens. Environ.*, vol. 112, pp. 2804–2816, Jun. 2008.

[72] B. Geiger, D. Carrer, L. Franchistéguy, J. L. Roujean, and C. Meurey, "Land surface albedo derived on a daily basis from Meteosat Second Generation observations," *IEEE Trans. Geosci. Remote Sens.*, vol. 46, pp. 3841–3856, 2008.

[73] C. Schaaf, J. Martonchik, B. Pinty, Y. Govaerts, F. Gao, A. Lattanzio, J. Liu, A. Strahler, and M. Taberner, "Retrieval of surface albedo from satellite sensors," in *Advances in Land Remote Sensing: System, Modeling, Inversion and Application*, S. Liang, Ed. New York: Springer, 2008, ch. 9, pp. 219–243.

[74] Y. M. Govaerts, B. Pinty, M. Taberner, and A. Lattanzio, "Spectral conversion of surface albedo derived from meteosat first generation observations," *IEEE Geosci. Remote Sens. Lett.*, vol. 3, pp. 23–27, Jan. 2006.

[75] W. J. D. van Leeuwen and J. L. Roujean, "Land surface albedo from the synergistic use of polar (EPS) and geo-stationary (MSG) observing systems—An assessment of physical uncertainties," *Remote Sens. Environ.*, vol. 81, pp. 273–289, Aug. 2002.

[76] S. Liang, "A direct algorithm for estimating land surface broadband albedos from MODIS imagery," *IEEE Trans. Geosci. Remote Sens.*, vol. 41, pp. 136–145, 2003.

[77] P. C. D. Milly and A. B. Shmakin, "Global modeling of land water and energy balances. Part I: The land dynamics (LaD) model," *J. Hydrometeorol.*, vol. 3, pp. 283–299, Jun. 2002.

[78] R. E. Dickinson, B. Pinty, and M. M. Verstraete, "Relating surface albedos in GCM to remotely sensed data," *Agricultur. Forest Meteorol.*, vol. 52, pp. 109–131, 1990.

[79] G. B. Bonan, K. W. Oleson, M. Vertenstein, S. Levis, X. Zeng, Y. Dai, R. E. Dickinson, and Z. L. Yang, "The land surface climatology of the community land model coupled to the NCAR community climate model," *J. Climate*, vol. 15, pp. 3123–3149, 2002.

[80] P. Sellers, "Canopy reflectance, photosynthesis and transpiration," *Int. J. Remote Sens.*, vol. 6, pp. 1335–1372, 1985.

[81] L. Zhou, R. E. Dickinson, Y. Tian, X. Zeng, Y. Dai, Z. L. Yang, C. B. Schaaf, F. Gao, Y. Jin, A. Strahler, R. B. Myneni, H. Yu, W. Wu, and M. Shaikh, "Comparison of seasonal and spatial variations of albedos from Moderate-Resolution Imaging Spectroradiometer (MODIS) and common land model," *J. Geophys. Res.*, vol. 108, p. 4488, 2003, 10.1029/2002JD003326.

[82] K. W. Oleson, G. B. Bonan, C. Schaaf, F. Gao, Y. F. Jin, and A. Strahler, "Assessment of global climate model land surface albedo using MODIS data," *Geophys. Res. Lett.*, vol. 30, p. 4, Apr. 2003.

[83] T. Matsui, A. Beltran-Przekurat, R. A. Pielke, D. Niyogi, and M. B. Coughenour, "Continental-scale multiobservation calibration and assessment of Colorado State University Unified Land Model by application of Moderate Resolution Imaging Spectroradiometer (MODIS) surface albedo," *J. Geophys. Res.-Biogeosci.*, vol. 112, p. 19, Jun. 2007.

[84] S. Wang, A. P. Trishchenko, K. V. Khlopenkov, and A. Davidson, "Comparison of International Panel on Climate Change Fourth Assessment Report climate model simulations of surface albedo with satellite products over northern latitudes," *J. Geophys. Res.*, vol. 111, 2006, Art. No. D21108.

[85] X. Zhang, S. Liang, K. Wang, L. Li, and S. Gui, "Analysis of global land surface shortwave broadband albedo from multiple data sources," *IEEE J. Special Topics Appl. Earth Observations Remote Sens.*, 2010, this issue.

[86] C. J. Houldcroft, W. M. F. Grey, M. Barnsley, C. M. Taylor, S. O. Los, and P. R. J. North, "New vegetation albedo parameters and global fields of soil background albedo derived from MODIS for use in a climate model," *J. Hydrometeorol.*, vol. 10, pp. 183–198, Feb. 2009.

[87] Z. Wang, X. Zeng, and M. Barlage, "Moderate resolution imaging spectroradiometer bidirectional reflectance distribution function-based albedo parameterization for weather and climate models," *J. Geophys. Res.–Atmospheres*, vol. 112, p. 16, Jan. 2007.

[88] X. Z. Liang, M. Xu, W. Gao, K. Kunkel, J. Slusser, Y. J. Dai, Q. L. Min, P. R. Houser, M. Rodell, C. B. Schaaf, and F. Gao, "Development of land surface albedo parameterization based on Moderate Resolution Imaging Spectroradiometer (MODIS) data," *J. Geophys. Res.–Atmospheres*, vol. 110, p. 22, Jun. 2005.

[89] D. Rechid, T. Raddatz, and D. Jacob, "Parameterization of snow-free land surface albedo as a function of vegetation phenology based on MODIS data and applied in climate modelling," *Theoret. Appl. Climatol.*, vol. 95, pp. 245–255, Mar. 2009.

[90] R. E. Dickinson, L. M. Zhou, Y. H. Tian, Q. Liu, T. Lavergne, B. Pinty, C. B. Schaaf, and Y. Knyazikhin, "A three-dimensional analytic model for the scattering of a spherical bush," *J. Geophys. Res.–Atmospheres*, vol. 113, p. 8, Oct. 2008.

[91] G. R. Diak, J. R. Mecikalski, M. C. Anderson, J. M. Norman, W. P. Kustas, R. D. Torn, and R. L. DeWolf, "Estimating land surface energy budgets from space—Review and current efforts at the University of Wisconsin-Madison and USDA-ARS," *Bull. Amer. Meteorol. Soc.*, vol. 85, pp. 65–78, Jan. 2004.

[92] R. G. Ellingson, "Surface longwave fluxes from satellite observations: A critical review," *Remote Sens. Environ.*, vol. 51, pp. 89–97, 1995.

[93] J. H. Kjaersgaard, F. L. Plauborg, and S. Hansen, "Comparison of models for calculating daytime long-wave irradiance using long term data set," *Agricultur. Forest Meteorol.*, vol. 143, pp. 49–63, Mar. 2007.

[94] G. N. Flerchinger, W. Xaio, D. Marks, T. J. Sauer, and Q. Yu, "Comparison of algorithms for incoming atmospheric long-wave radiation," *Water Resources Res.*, vol. 45, p. 13, Mar. 2009.

[95] S. W. Seemann, J. Li, W. P. Menzel, and L. E. Gumley, "Operational retrieval of atmospheric temperature, moisture, and ozone from MODIS infrared radiances," *J. Appl. Meteorol.*, vol. 42, pp. 1072–1091, Aug. 2003.

[96] W. Wang and S. Liang, "Estimating high-spatial resolution clear-sky land surface downwelling and net longwave radiation from MODIS data," *Remote Sens. Environ.*, vol. 113, pp. 745–754, 2009.

[97] H. T. Lee and R. G. Ellingson, "Development of a nonlinear statistical method for estimating the downward longwave radiation at the surface from satellite observations," *J. Atmospher. Ocean. Technol.*, vol. 19, pp. 1500–1515, Oct. 2002.

[98] W. Wang and S. Liang, "A method for estimating clear-sky instantaneous land surface longwave radiation from GOES sounder and GOES-R ABI data," *IEEE Geosci. Remote Sens. Lett.*, 2010, in press.

[99] M. Wild, A. Ohmura, H. Gilgen, and E. Roeckner, "Validation of general-circulation model radiative fluxes using surface observations," *J. Climate*, vol. 8, pp. 1309–1324, May 1995.

[100] J. R. Garratt and A. J. Prata, "Downwelling longwave fluxes at continental surfaces—A comparison of observations with GCM simulations and implications for the global land surface radiation budget," *J. Climate*, vol. 9, pp. 646–655, Mar. 1996.

[101] J. J. Morcrette, "The surface downward longwave radiation in the ECMWF forecast system," *J. Climate*, vol. 15, pp. 1875–1892, Jul. 2002.

[102] M. Markovic, C. G. Jones, P. A. Vaillancourt, D. Paquin, K. Winger, and D. Paquin-Ricard, "An evaluation of the surface radiation budget over North America for a suite of regional climate models against surface station observations," *Climate Dynamics*, vol. 31, pp. 779–794, Dec. 2008.

[103] M. J. Iacono, E. J. Mlawer, S. A. Clough, and J. J. Morcrette, "Impact of an improved longwave radiation model, RRTM, on the energy budget and thermodynamic properties of the NCAR community climate model, CCM3," *J. Geophys. Res.–Atmospheres*, vol. 105, pp. 14873–14890, Jun. 2000.

[104] M. Wild, A. Ohmura, H. Gilgen, J. J. Morcrette, and A. Slingo, "Evaluation of downward longwave radiation in general circulation models," *J. Climate*, vol. 14, pp. 3227–3239, 2001.

[105] F. Prata, "The Climatological Record of Clear-Sky Longwave Radiation at the Earth's Surface: Evidence for Water Vapour Feedback?" 2008, pp. 5247–5263.

[106] M. Jin and S. Liang, "Improve land surface emissivity parameter for land surface models using global remote sensing observations," *J. Climate*, vol. 19, pp. 2867–2881, 2006.

[107] K. Ogawa, T. Schmugge, F. Jacob, and A. French, "Estimation of broadband land surface emissivity from multispectral thermal infrared remote sensing," *Agronomie*, vol. 22, pp. 695–696, 2002.

[108] K. Wang, Z. Wan, P. Wang, M. Sparrow, and J. Liu, "Estimation of land surface upwelling long wave radiation and broadband emissivity using MODIS LST products," *J. Geophys. Res.–Atmospheres*, vol. 110, p. D11109, 2005, 10.1029/2004JD005566.

[109] A. R. Gillespie, S. Rokugawa, T. Matsunaga, J. Cothern, S. Hook, and A. Kahle, "A temperature and emissivity separation algorithm for Advanced Spaceborne Thermal Emission and Reflection Radiometer (ASTER) images," *IEEE Trans. Geosci. Remote Sens.*, vol. 36, pp. 1113–1126, 1998.

[110] Z. M. Wan, "New refinements and validation of the MODIS land-surface temperature/emissivity products," *Remote Sens. Environ.*, vol. 112, pp. 59–74, Jan. 2008.

[111] S. Liang, "Recent developments in estimating land surface biogeophysical variables from optical remote sensing," *Progr. Phys. Geography*, vol. 31, pp. 501–516, Oct. 2007.

[112] W. Wang, S. Liang, and T. Meyer, "Validating MODIS land surface temperature products," *Remote Sens. Environ.*, vol. 112, pp. 623–635, 2008.

[113] G. C. Hulley and S. J. Hook, "Intercomparison of versions 4, 4.1 and 5 of the MODIS land surface temperature and emissivity products and validation with laboratory measurements of sand samples from the Namib desert, Namibia," *Remote Sens. Environ.*, vol. 113, pp. 1313–1318, Jun. 2009.

[114] K. Wang and S. Liang, "Evaluation of ASTER and MODIS land surface temperature and emissivity products using surface longwave radiation observations at SURFRAD sites," *Remote Sens. Environ.*, vol. 113, pp. 1156–1165, 2009.

[115] J. Cheng, S. Liang, J. Wang, and X. Li, "A stepwise refining algorithm of temperature and emissivity separation for hyperspectral thermal infrared data," *IEEE Trans. Geosci. Remote Sens.*, vol. 48, pp. 1588–1597, 2010.

[116] F. Karbou, E. Gerard, and F. Rabier, "Microwave land emissivity and skin temperature for AMSU-A and -B assimilation over land," *Quarterly J. Royal Meteorol. Soc.*, vol. 132, pp. 2333–2355, Oct. 2006.

[117] W. Wang, S. Liang, and J. A. Augustine, "Estimating clear-sky land surface longwave upwelling radiation from MODIS data," *IEEE Trans. Geosci. Remote Sens.*, vol. 47, pp. 1555–1570, 2009.

[118] Y. C. Zhang, W. B. Rossow, and P. W. Stackhouse, "Comparison of different global information sources used in surface radiative flux calculation: Radiative properties of the surface," *J. Geophys. Res.–Atmospheres*, vol. 112, p. 20, Jan. 2007.

[119] S. K. Gupta, A. C. Wilber, W. L. Darnell, and J. T. Suttles, "Longwave surface radiation over the globe from satellite data—An error analysis," *Int. J. Remote Sens.*, vol. 14, pp. 95–114, Jan. 1993.

[120] G. R. Diak, J. R. Mecikalski, M. C. Anderson, J. M. Norman, W. P. Kustas, R. D. Torn, and R. L. DeWolf, "Estimating land surface energy budgets from space—Review and current efforts at the University of Wisconsin-Madison and USDA-ARS," *Bull. Amer. Meteorol. Soc.*, vol. 85, p. 65, Jan. 2004.

[121] J. P. Lhomme, J. J. Vacher, and A. Rocheteau, "Estimating downward long-wave radiation on the Andean Altiplano," *Agricultur. Forest Meteorol.*, vol. 145, pp. 139–148, Aug. 2007.

[122] M. G. Iziomon, H. Mayer, and A. Matzarakis, "Downward atmospheric longwave irradiance under clear and cloudy skies: Measurement and parameterization," *J. Atmospher. Solar-Terrestr. Phys.*, vol. 65, pp. 1107–1116, Jul. 2003.

[123] G. R. Diak, W. L. Bland, J. R. Mecikalski, and M. C. Anderson, "Satellite-based estimates of longwave radiation for agricultural applications," *Agricultur. Forest Meteorol.*, vol. 103, pp. 349–355, Jul. 1, 2000.

[124] K. Wang and S. Liang, "Estimation of surface net radiation from solar shortwave radiation measurements," *J. Appl. Meteorol. Climatol.*, vol. 48, pp. 634–643, 2009.

[125] T. T. Shi, D. X. Guan, J. B. Wu, A. Z. Wang, C. J. Jin, and S. J. Han, "Comparison of methods for estimating evapotranspiration rate of dry forest canopy: Eddy covariance, Bowen ratio energy balance, and Penman-Monteith equation," *J. Geophys. Res.–Atmospheres*, vol. 113, p. 15, Oct. 2008.

[126] V. R. N. Pauwels and R. Samson, "Comparison of different methods to measure and model actual evapotranspiration rates for a wet sloping grassland," *Agricultur. Water Manage.*, vol. 82, pp. 1–24, Apr. 2006.

[127] K. Wilson, A. Goldstein, E. Falge, M. Aubinet, D. Baldocchi, P. Berbigier, C. Bernhofer, R. Ceulemans, H. Dolman, C. Field, A. Grelle, A. Ibrom, B. E. Law, A. Kowalski, T. Meyers, J. Moncrieff, R. Monson, W. Oechel, J. Tenhunen, R. Valentini, and S. Verma, "Energy Balance Closure at FLUXNET Sites," 2002, pp. 223–243.

[128] T. E. Twine, W. P. Kustas, J. M. Norman, D. R. Cook, P. R. Houser, T. P. Meyers, J. H. Prueger, P. J. Starks, and M. L. Wesely, "Correcting eddy-covariance flux underestimates over a grassland," *Agricultur. Forest Meteorol.*, vol. 103, pp. 279–300, Jun. 2000.

[129] T. Foken, "The energy balance closure problem: An overview," *Ecol. Applicat.*, vol. 18, pp. 1351–1367, Sep. 2008.

[130] A. G. Barr, A. K. Betts, R. L. Desjardins, and J. I. MacPherson, "Comparison of regional surface fluxes from boundary-layer budgets and aircraft measurements above boreal forest," *J. Geophys. Res.–Atmospheres*, vol. 102, pp. 29213–29218, Dec. 1997.

[131] R. G. Anderson and M. L. Goulden, "A mobile platform to constrain regional estimates of evapotranspiration," *Agricultur. Forest Meteorol.*, vol. 149, pp. 771–782, May 2009.
[132] J. Kleissl, S. H. Hong, and J. M. H. Hendrickx, "New Mexico scintillometer network supporting remote sensing and hydrologic and meteorological models," *Bull. Amer. Meteorol. Soc.*, vol. 90, p. 207, Feb. 2009.
[133] E. P. Glenn, A. R. Huete, P. L. Nagler, K. K. Hirschboeck, and P. Brown, "Integrating remote sensing and ground methods to estimate evapotranspiration," *Critical Rev. Plant Sci.*, vol. 26, pp. 139–168, 2007.
[134] J. D. Kalma, T. R. McVicar, and M. F. McCabe, "Estimating land surface evaporation: A review of methods using remotely sensed surface temperature data," *Surveys Geophys.*, vol. 29, pp. 421–469, Oct. 2008.
[135] Z. L. Li, R. L. Tang, Z. M. Wan, Y. Y. Bi, C. H. Zhou, B. H. Tang, G. J. Yan, and X. Y. Zhang, "A review of current methodologies for regional evapotranspiration estimation from remotely sensed data," *Sensors*, vol. 9, pp. 3801–3853, May 2009.
[136] H. J. Farahani, T. A. Howell, W. J. Shuttleworth, and W. C. Bausch, "Evapotranspiration: Progress in measurement and modeling in agriculture," *Trans. Asabe*, vol. 50, pp. 1627–1638, Sep.–Oct. 2007.
[137] P. L. Nagler, E. P. Glenn, H. Kim, W. Emmerich, R. L. Scott, T. E. Huxman, and A. R. Huete, "Relationship between evapotranspiration and precipitation pulses in a semiarid rangeland estimated by moisture flux towers and MODIS vegetation indices," *J. Arid Environ.*, vol. 70, pp. 443–462, Aug. 2007.
[138] T. Carlson, "An overview of the "triangle method" for estimating surface evapotranspiration and soil moisture from satellite imagery," *Sensors*, vol. 7, pp. 1612–1629, Aug. 2007.
[139] F. H. Yang, M. A. White, A. R. Michaelis, K. Ichii, H. Hashimoto, P. Votava, A. X. Zhu, and R. R. Nemani, "Prediction of continental-scale evapotranspiration by combining MODIS and AmeriFlux data through support vector machine," *IEEE Trans. Geosci. Remote Sens.*, vol. 44, pp. 3452–3461, Nov. 2006.
[140] J. B. Fisher, K. P. Tu, and D. D. Baldocchi, "Global estimates of the land-atmosphere water flux based on monthly AVHRR and ISLSCP-II data, validated at 16 FLUXNET sites," *Remote Sens. Environ.*, vol. 112, pp. 901–919, Mar. 2008.
[141] Q. Mu, F. A. Heinsch, M. Zhao, and S. W. Running, "Development of a global evapotranspiration algorithm based on MODIS and global meteorology data," *Remote Sens. Environ.*, vol. 111, pp. 519–536, Dec. 2007.
[142] H. A. Cleugh, R. Leuning, Q. Z. Mu, and S. W. Running, "Regional evaporation estimates from flux tower and MODIS satellite data," *Remote Sens. Environ.*, vol. 106, pp. 285–304, Feb. 2007.
[143] W. P. Kustas, A. N. French, J. L. Hatfield, T. J. Jackson, M. S. Moran, A. Rango, J. C. Ritchie, and T. J. Schmugge, "Remote sensing research in hydrometeorology," *Photogramm. Eng. Remote Sens.*, vol. 69, pp. 631–646, Jun. 2003.
[144] J. Overgaard, D. Rosbjerg, and M. B. Butts, "Land-surface modelling in hydrological perspective—A review," *Biogeosciences*, vol. 3, pp. 229–241, 2006.
[145] R. G. Allen, M. Tasumi, and R. Trezza, "Satellite-based energy balance for mapping evapotranspiration with internalized calibration (METRIC)—Model," *J. Irrigat. Drain. Eng.–ASCE*, vol. 133, pp. 380–394, Jul.–Aug. 2007.
[146] W. G. M. Bastiaanssen, E. J. M. Noordman, H. Pelgrum, G. Davids, B. P. Thoreson, and R. G. Allen, "SEBAL model with remotely sensed data to improve water-resources management under actual field conditions," *J. Irrigat. Drain. Eng.–ASCE*, vol. 131, pp. 85–93, Jan.–Feb. 2005.
[147] K. Nishida, R. R. Nemani, S. W. Running, and J. M. Glassy, "An operational remote sensing algorithm of land surface evaporation," *J. Geophys. Res.*, vol. 108, 2003, Art. #4270.
[148] M. Pan, E. F. Wood, R. Wojcik, and M. F. McCabe, "Estimation of regional terrestrial water cycle using multi-sensor remote sensing observations and data assimilation," *Remote Sens. Environ.*, vol. 112, pp. 1282–1294, Apr. 2008.
[149] J. Qin, S. Liang, R. Liu, H. Zhang, and B. Hu, "A weak-constraint based data assimilation scheme for estimating surface turbulent fluxes," *IEEE Geosci. Remote Sens. Lett.*, vol. 4, pp. 649–653, 2007.
[150] M. F. McCabe, E. F. Wood, R. Wojcik, M. Pan, J. Sheffield, H. Gao, and H. Su, "Hydrological consistency using multi-sensor remote sensing data for water and energy cycle studies," *Remote Sens. Environ.*, vol. 112, pp. 430–444, Feb. 2008.
[151] J. Sheffield, C. R. Ferguson, T. J. Troy, E. F. Wood, and M. F. McCabe, "Closing the terrestrial water budget from satellite remote sensing," *Geophys. Res. Lett.*, vol. 36, p. 5, Apr. 2009.
[152] S. Swenson and J. Wahr, "Monitoring the water balance of Lake Victoria, East Africa, from space," *J. Hydrol.*, vol. 370, pp. 163–176, May 2009.
[153] T. H. Syed, J. S. Famiglietti, and D. P. Chambers, "GRACE-based estimates of terrestrial freshwater discharge from basin to continental scales," *J. Hydrometeorol.*, vol. 10, pp. 22–40, Feb. 2009.
[154] G. Ramillien, J. S. Famiglietti, and J. Wahr, "Detection of continental hydrology and glaciology signals from GRACE: A review," *Surveys Geophys.*, vol. 29, pp. 361–374, Oct. 2008.
[155] G. J. Huffman, R. F. Adler, D. T. Bolvin, G. J. Gu, E. J. Nelkin, K. P. Bowman, Y. Hong, E. F. Stocker, and D. B. Wolff, "The TRMM multisatellite precipitation analysis (TMPA): Quasi-global, multiyear, combined-sensor precipitation estimates at fine scales," *J. Hydrometeorol.*, vol. 8, pp. 38–55, Feb. 2007.
[156] R. J. Joyce, J. E. Janowiak, P. A. Arkin, and P. P. Xie, "CMORPH: A method that produces global precipitation estimates from passive microwave and infrared data at high spatial and temporal resolution," *J. Hydrometeorol.*, vol. 5, pp. 487–503, Jun. 2004.
[157] D. E. Alsdorf and D. P. Lettenmaier, "Tracking fresh water from space," *Science*, vol. 301, p. 1491, Sep. 2003.
[158] W. J. Shuttleworth, "Putting the 'vap' into evaporation," *Hydrol. Earth Syst. Sci.*, vol. 11, pp. 210–244, 2007.
[159] A. Robock, L. F. Luo, E. F. Wood, F. H. Wen, K. E. Mitchell, P. R. Houser, J. C. Schaake, D. Lohmann, B. Cosgrove, J. Sheffield, Q. Y. Duan, R. W. Higgins, R. T. Pinker, J. D. Tarpley, J. B. Basara, and K. C. Crawford, "Evaluation of the North American Land Data Assimilation System over the southern Great Plains during the warm season," *J. Geophys. Res.–Atmospheres*, vol. 108, p. 21, Nov. 2003.
[160] D. Waliser, K. W. Seo, S. Schubert, and E. Njoku, "Global water cycle agreement in the climate models assessed in the IPCC AR4," *Geophys. Res. Lett.*, vol. 34, p. 6, Aug. 2007.
[161] C. A. Schlosser and P. R. Houser, "Assessing a satellite-era perspective of the global water cycle," *J. Climate*, vol. 20, pp. 1316–1338, Apr. 2007.
[162] R. Grotjahn, "Different data, different general circulations? A comparison of selected fields in NCEP/DOE AMIP-II and ECMWF ERA-40 reanalyses," *Dynamics of Atmospheres and Oceans*, vol. 44, pp. 108–142, Mar. 2008.
[163] K. E. Trenberth, J. T. Fasullo, and J. Kiehl, "Earth's global energy budget," *Bull. Amer. Meteorol. Soc.*, vol. 90, p. 311, Mar. 2009.
[164] P. A. Dirmeyer, C. A. Schlosser, and K. L. Brubaker, "Precipitation, recycling, and land memory: An integrated analysis," *J. Hydrometeorol.*, vol. 10, pp. 278–288, Feb. 2009.
[165] P. A. Dirmeyer, X. A. Gao, M. Zhao, Z. C. Guo, T. K. Oki, and N. Hanasaki, "GSWP-2—Multimodel anlysis and implications for our perception of the land surface," *Bull. Amer. Meteorol. Soc.*, vol. 87, p. 1381, Oct. 2006.
[166] Y. Yao, S. Liang, Q. Qin, K. Wang, and S. Zhao, "Mmodelonitoring global land surface drought based on an improved evapotranspiration," *IEEE J. Special Topics Appl. Earth Observations Remote Sens.*, 2010, submitted.
[167] T. C. Peterson, V. S. Golubev, and P. Y. Groisman, "Evaporation losing its strength," *Nature*, vol. 377, pp. 687–688, Oct. 1995.
[168] M. T. Hobbins, J. A. Ramirez, and T. C. Brown, "Trends in pan evaporation and actual evapotranspiration across the conterminous US: Paradoxical or complementary?," *Geophys. Res. Lett.*, vol. 31, p. 5, Jul. 2004.
[169] M. L. Roderick and G. D. Farquhar, "The cause of decreased pan evaporation over the past 50 years," *Science*, vol. 298, pp. 1410–1411, Nov. 2002.
[170] M. L. Roderick, L. D. Rotstayn, G. D. Farquhar, and M. T. Hobbins, "On the attribution of changing pan evaporation," *Geophys. Res. Lett.*, vol. 34, p. 6, Sep. 2007.
[171] Z. T. Cong, D. W. Yang, and G. H. Ni, "Does evaporation paradox exist in China?," *Hydrol. Earth Syst. Sci.*, vol. 13, pp. 357–366, 2009.
[172] L. J. Gordon, W. Steffen, B. F. Jonsson, C. Folke, M. Falkenmark, and A. Johannessen, "Human modification of global water vapor flows from the land surface," *Proc. Nat. Acad. Sci. USA*, vol. 102, pp. 7612–7617, May 2005.
[173] G. Gao, D. L. Chen, C. Y. Xu, and E. Simelton, "Trend of estimated actual evapotranspiration over China during 1960–2002," *J. Geophys. Res.–Atmospheres*, vol. 112, p. 8, Jun. 2007.
[174] M. J. Czikowsky and D. R. Fitzjarrald, "Evidence of seasonal changes in evapotranspiration in eastern US hydrological records," *J. Hydrometeorol.*, vol. 5, pp. 974–988, Oct. 2004.
[175] M. T. Walter, D. S. Wilks, J. Y. Parlange, and R. L. Schneider, "Increasing evapotranspiration from the conterminous United States," *J. Hydrometeorol.*, vol. 5, pp. 405–408, Jun. 2004.

[176] W. Brutsaert, “Indications of increasing land surface evaporation during the second half of the 20th century,” *Geophys. Res. Lett.*, vol. 33, p. 4, Oct. 2006.

[177] A. J. Teuling, M. Hirschi, A. Ohmura, M. Wild, M. Reichstein, P. Ciais, N. Buchmann, C. Ammann, L. Montagnani, A. D. Richardson, G. Wohlfahrt, and S. I. Seneviratne, “A regional perspective on trends in continental evaporation,” *Geophys. Res. Lett.*, vol. 36, p. 5, Jan. 2009.

[178] M. Wild, “Solar radiation budgets in atmospheric model intercomparisons from a surface perspective,” *Geophys. Res. Lett.*, vol. 32, p. 4, Apr. 2005.

Shunlin Liang (M’94–SM’01) received the Ph.D. degree in remote sensing and GIS from Boston University, Boston, MA.

He was a Postdoctoral Research Associate with Boston University from 1992 to 1993 and a Validation Scientist with the NOAA/NASA Pathfinder AVHRR Land Project from 1993 to 1994. He is currently a Professor with the University of Maryland, College Park. His main research interests focus on spatio-temporal analysis of remotely sensed data, integration of data from different sources and numerical models, and linkage of remote sensing with global environmental changes. He authored the book *Quantitative Remote Sensing of Land Surfaces* (Wiley, 2004) and edited the book *Advances in Land Remote Sensing: System, Modeling, Inversion and Application* (Springer, 2008).

Dr. Liang is a member of NASA ASTER and MODIS science teams and NOAA GOES-R Land science team. He is a co-chairman of the International Society for Photogrammetry and Remote Sensing Commission VII/I Working Group on Fundamental Physics and Modeling. He is an Associate Editor of the IEEE TRANSACTIONS ON GEOSCIENCE AND REMOTE SENSING, subject editor of the *Annals of GIS*, and also a guest editor of several remote sensing journals.

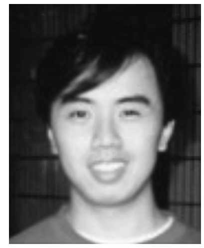

Kaicun Wang received the Ph.D. degree in atmospheric sciences from Peking University, China, in 2004.

He is a Research Scientist Associate V in the Department of Geological Science, University of Texas at Austin. He held an assistant researcher position at the Institute of Atmospheric Physics, from 2004 to 2006. From July 2006 to November 2009, he worked at the Department of Geography, University of Maryland as a Research Associate to Research Assistant Professor. His research interests focus on surface net radiation, global evapotranspiration, air pollution and global climate change. He created reliable estimates of global aerosol optical depth, incident solar radiation and evapotranspiration over the land during past several decades. He is the leading author of more than 30 peer-reviewed journal papers, in such journals as *Science*. He serves as a peer reviewer for more than 15 international journals in climate and remote sensing.

Xiaotong Zhang is currently pursuing the Ph.D. degree at Wuhan University, China.

He was a Faculty Research Assistant with the University of Maryland from 2008 to 2010. He received a Masters degree in cartography and geographic information science from Wuhan University, China in 2006. His present research interests focus on the algorithms for retrieving surface radiation products from multiple satellites data.

Martin Wild is a Senior Scientist at the Swiss Federal Institute of Technology (ETH Zurich), Switzerland. His expertise lies in working with both global climate models (GCMs) and comprehensive observational datasets, as documented in more than 80 peer-reviewed publications and two IPCC reports. His major research interests are related to the global energy and water cycles, with emphasis on the radiation, energy and water fluxes at the Earth’s surface. A particular focus is on the decadal variations of these components (e.g., global dimming and brightening) and related consequences for the climate system and climate change, as well as their representation in climate models. Recently he acted as guest editor for a special issue on global dimming and brightening in the *Journal of Geophysical Research*, and is now an associate editor with the same journal. He also chairs the working group on the global energy balance of the International Radiation Commission (IRC).